Environmental Science
Advances

ROYAL SOCIETY
OF CHEMISTRY

PAPER

View Article Online
View Journal | View Issue

Check for updates

Cite this: *Environ. Sci.: Adv.*, 2026, **5**, 1594

# Efficient Fenton/biological activated carbon filter process for treating landfill leachates

Dongxu Zhou,[a] Salma Tabassum, *[bc] Jun Li,*[a] Li Zhang,[a] Ningwen Zhang,[a] Guanglei Li,[a] Hüseyin Altundag[bc] and Imran Khan [d]

Received 10th February 2026
Accepted 30th March 2026

DOI: 10.1039/d6va00072j

rsc.li/esadvances

The treatment of landfill leachates is considered to be one of the most difficult processes among organic wastewater treatments. This study aims to address the challenge of treating landfill leachates by developing a new combined Fenton/biological activated carbon filter process to efficiently treat organic matter, ammonia nitrogen ($NH_4^+$-N), and chromaticity. Under optimal Fenton process conditions (pH 4, $H_2O_2$ dosage of 15 mL $L^{-1}$, $n(H_2O_2):n(Fe^{2+}) = 4:1$, and reaction time of 100 min), the removal efficiencies of COD, chromaticity, and $NH_4^+$-N reached 75.05%, 98.32%, and 30%, respectively. Response surface methodology confirmed that the significance of influencing factors follow the order of pH > $H_2O_2$ dosage > $n(H_2O_2):n(Fe^{2+})$ > reaction time, with a verified COD removal efficiency of 74.36% (minimal error). For the SPC/$Fe^{2+}$ process, optimal conditions yielded COD, chromaticity, and $NH_4^+$-N removal efficiencies of 58.39%, 84.21%, and 20.30%, respectively. The BAC filter achieved effective COD removal (27.3%) and excellent $NH_4^+$-N removal (61.90%). The Fenton/BAC combined process achieved a remarkable treatment performance for landfill leachate, with a COD removal efficiency of 81.86%, $NH_4^+$-N removal efficiency of 73.33%, and chromaticity removal efficiency of 98.50%. Notably, the biodegradability index (B/C) of the landfill leachate increased from 0.31 to 0.51, confirming the synergistic mechanism of organic matter and $NH_4^+$-N removal by BAC. This study innovatively constructs a Fenton/BAC combined process, quantifies the synergistic removal effects of adsorption-biofilm-microbial degradation by BAC on leachate organics and $NH_4^+$-N, and clarifies the SPC/$Fe^{2+}$-Fenton performance-cost trade-off, providing a new technical route for efficient leachate treatment. This novel combined process offers promising research directions and significant theoretical and practical value for efficient leachate treatment.

**Environmental significance**

The primary hazards of landfill leachates to their surrounding environment include soil, groundwater, and atmospheric pollution, as well as the eutrophication of water bodies. Existing research primarily employs either single physicochemical or biological methods. However, their treatment effects are often suboptimal and fail to achieve the expected degradation. This study proposes a Fenton/biological activated carbon filter combined process for efficient landfill leachate treatment. A dual-dimensional analysis of performance and cost showed that the Fenton/BAC combined process had the lowest cost per unit of pollutant removal. It exhibited superior overall competitiveness compared with single Fenton or SPC/$Fe^{2+}$ processes, addressing the limitations of single performance or cost analyses in existing related studies. This is a new process with promising research directions, both theoretically and practically significant, for achieving efficient leachate treatment.

## 1. Introduction

With the steady improvement of the economy and living standards, the amount of urban domestic waste generated is also gradually increasing.[1,2] Organic waste accounts for 50% to 70% of the total waste weight. Landfills have some advantages and are a solid waste treatment technology, but the high concentration of leachates they produce can cause severe environmental pollution.[3] As landfill time increases, leachates will continue to pollute the soil, groundwater, surface water, and other water bodies. This leads to a deterioration in water quality, which may persist for decades to centuries.[4] In areas with higher rainfall, the content of organic compounds is higher.[5] The pollutants in leachates include inorganic components, dissolved organic matter, and organic matter generated by residential life and chemical production.[6,7] Landfill leachates

---

[a] *School of Municipal and Environmental Engineering, Shenyang Jianzhu University, Shenyang 110168, China. E-mail: junlee@sjzu.edu.cn*
[b] *Department of Chemistry, Faculty of Science, Sakarya University, Sakarya 54187, Turkey. E-mail: tsalma@sakarya.edu.tr; salmazenith@gmail.com*
[c] *Biomedical, Magnetic and Semiconductor Materials Research Center (BIMAS-RC), Sakarya University, Sakarya 54187, Turkey*
[d] *Department of Chemistry, College of Science, Sultan Qaboos University, Muscat, Oman*

exhibit high pollutant concentrations, high organic pollutant content, complex composition, and severely imbalanced nutrient proportions for microorganisms, resulting in significant changes in water quality and elevated metal levels.[8] To address the core technical bottlenecks in landfill leachate treatment, including poor biodegradability, low ammonia nitrogen removal efficiency of single advanced oxidation processes (*e.g.*, Fenton process), and the tendency for traditional biological activated carbon (BAC) to adsorb and saturate without pretreatment, this study proposes a combined process strategy. It systematically explores the synergistic mechanism for removing organic matter and ammonia nitrogen. The primary hazards of landfill leachates to the surrounding environment include soil, groundwater, and atmospheric pollution and the eutrophication of water bodies.[9,10] Various factors influence the water quality of landfill leachates, and the indicators of water quality are affected accordingly.[11,12] Consequently, the treatment effect of a single physicochemical or biological method is not ideal. Moreover, landfill leachates contain a variety of heavy metals, endocrine-disrupting hormones, pesticides, halogenated organic compounds, and other trace pollutants. These trace pollutants are carcinogenic and teratogenic, posing a serious threat to our health.[13] Because the high concentration of pollutants in landfill leachates can cause specific toxicity to microorganisms, it cannot provide conditions for their growth and reproduction, making it impossible to use biological treatment processes to treat landfill leachates alone and thus failing to meet discharge requirements. In China, the treatment cost of landfill leachates is typically 8–15 USD per $m^3$, and traditional processes (*e.g.*, single Fenton process and activated carbon adsorption) often face problems, such as high chemical consumption, frequent adsorbent replacement, and difficulty in meeting increasingly stringent discharge standards.[9,13] This study targets the practical engineering issues of high cost, complex operation, and poor deep-treatment effects of leachates. It develops a combined Fenton/BAC process that is economically feasible and operationally convenient, with important practical significance for promoting the efficient, low-cost treatment of landfill leachates.

Physicochemical treatment methods are often set before biological treatment methods. However, the treatment costs of these methods are generally high and their operational and management requirements are also strict.[14–16] Thus, researchers have begun to conduct in-depth research on combined advanced oxidation processes, which improve treatment effects while also compensating for the shortcomings of individual oxidation technologies.[17] However, the interaction relationships and influence laws among various parameters in combined processes remain unclear. Therefore, the present study utilizes landfill leachate as the experimental subject and determines the suitable combined treatment process parameters for this type of wastewater through experimentation. In urban landfills, biological treatment is also one of the most widely used methods for treating landfill leachate; however, its treatment effect is unstable and easily influenced by external conditions.[18–20] The land treatment method removes suspended particles and dissolved substances from landfill leachate as it flows into the soil. However, this treatment method cannot remove heavy metals or toxic and harmful substances.[21,22] Integrating physical, chemical, and biological processes can compensate for the shortcomings of single processes[23] and combine the advantages of several treatment processes to amplify their benefits and enhance the overall treatment efficiency. This is also feasible in terms of economy and technology.[16,24]

The Fenton process is an advanced chemical oxidation process, which is generally carried out at pH 3–5.[25] The Fenton process can be used as a pretreatment, advanced treatment, or in combination with other methods. It is widely used for the pretreatment of toxic organic pollutants and for the advanced treatment of various types of wastewaters.[26,27] The Fenton process is used to remove pollutants from natural and industrial wastewater.[28,29] In comparison, sodium percarbonate (SPC), also known as dry hydrogen peroxide, has lower costs, a wider range of applicable temperatures, and a broader pH range than the Fenton reagent. It also exhibits good water solubility, is environmentally friendly, easy to transport, store, and measure, and non-corrosive.[30,31] SPC oxidation treatment is performed in wastewater treatment,[32,33] soil remediation,[34] drinking water purification,[35] *etc.*.[36] Advanced oxidation technologies based on SPC have been developed to improve the treatment efficiency.[37,38] When using chemical oxidation to treat landfill leachate, pollutant concentrations are reduced, and biodegradability is improved; however, the efficiency of ammonia nitrogen removal is low. To further reduce contaminant concentrations, bio-activated carbon filters can be used to treat the effluent.[39,40]

With the advancement of social development and increasingly stringent water quality requirements, bio-activated carbon (BAC) has been used in the refining steps of large-scale drinking water plants to remove taste and odour compounds and absorbable organic carbon.[41,42] BAC technology is also used in domestic sewage,[43] industrial wastewater,[44] oily wastewater,[45] coking wastewater,[46] pharmaceutical wastewater,[47] and radioactive wastewater[48] treatments. The primary application of biological activated carbon technology in actual wastewater treatment is the biological activated carbon filter. This technology seamlessly integrates traditional activated carbon with biological filtration, leveraging the strengths of both while mitigating their individual shortcomings. It is biofilm treatment technology that supports high hydraulic loadings and delivers good effluent quality. It effectively controls indicators such as organic matter, odor, and ammonia nitrogen in the water. The chemical oxygen demand (COD) adsorption capacity of BAC filters is 4- to 20-times that of activated carbon, significantly improving the adsorption capacity and removing ammonia nitrogen, chromaticity, and heavy metals, among other contaminants. Biological activated carbon filters can convert $NH_3$ into $NO_3^-$ and may also cause biological denitrification. However, activated carbon cannot convert $NH_3$ into $NO_3^-$ and has no adsorption capacity for it. The degradation effect of microorganisms effectively extends the operation and regeneration cycle of activated carbon, reducing operating costs. BAC has simple process equipment, high utilization efficiency, convenient management, stable operational performance, high removal efficiency, no sludge production, and is environmentally friendly.[49–51]

In recent years, chlorinated volatile organic compounds (CVOCs) with acute toxicity have received increasing attention, and these micropollutants have become prevalent in rivers. Kim *et al.*[52] studied the removal of organic carbon from river water through oxidation and activated carbon adsorption. The CVOC removal efficiency of BAC filters was 3–9-times that of powdered activated carbon (PAC), which had a removal efficiency of less than 20%. Ultimately, it was concluded that, regardless of the CVOC concentration in the influent, the system configuration of pre-ozonation, coagulation, sedimentation, sand filtration, post-ozonation, and BAC biological filter can almost completely remove CVOCs. This indicates that the combination of BAC filter and ozonation can provide an effective alternative to conventional chlorination and filtration processes for removing CVOCs.

Exploring novel combined physicochemical and biological treatment processes to achieve efficient leachate treatment is a promising research direction with both theoretical and practical significance. Despite the extensive application of Fenton oxidation, SPC/Fenton-like oxidation, and BAC combined processes in leachate treatment, current research still has critical gaps,[26,30,39–41] as follows: ① traditional Fenton processes primarily target organic pollutant degradation (*e.g.*, COD removal efficiency up to 70–80%[26,28]), but suffer from low $NH_4^+$-N removal (<30%[30]) and lack systematic optimization of parameter interactions (*e.g.*, pH, $H_2O_2$ dosage, and $Fe^{2+}$ ratio) *via* statistical methods such as RSM;[27] ② SPC/Fenton-like studies highlight their advantages in wider pH adaptability[36,37] but focus only on organic removal, lacking industrial-scale performance-cost comparison with the traditional Fenton process to guide engineering selection;[34] ③ existing Fenton/BAC combined processes have been confirmed to have a synergistic effect on pollutant removal,[39,41] but studies fail to quantify the individual contributions of activated carbon adsorption, biofilm adsorption, and microbial degradation in BAC and clarify how activated carbon dosage/type affect the treatment efficiency.[68] To fill these gaps, the key innovations of this study are: ① optimizing the Fenton process parameters *via* response surface methodology (RSM) and clarifying factor significance for COD removal; ② conducting comprehensive performance-cost comparison between SPC/Fenton and traditional Fenton processes for engineering application guidance; ③ quantifying the three-level removal contributions of BAC (activated carbon adsorption-biofilm adsorption-microbial degradation) for the first time, revealing the synergistic mechanism; and ④ systematically investigating the effects of activated carbon dosage/type to provide practical engineering parameters.

This study first utilized the Fenton advanced oxidation process to remove COD, color, and other indicators from the leachate and examines the factors that affect its level. The treatment effect of the sodium percarbonate (SPC)/$Fe^{2+}$ advanced oxidation process on the leachate and the factors affecting its level were compared. Then, these two advanced oxidation processes were optimized and the leachate was treated under the best conditions. Based on this, a combined Fenton/biological activated carbon filter process was developed to study its leachate treatment efficiency. Finally, the removal mechanisms of organic matter and ammonia nitrogen by the biological activated carbon filter were explored. The objectives were as follows: (i) studying the effects of four factors, reaction pH, $n(H_2O_2):n(Fe^{2+})$ ratio, $H_2O_2$ dosage, and reaction time, on the experiment by measuring the removal efficiency of COD and chromaticity to determine the optimal reaction conditions and treatment effect. The Fenton method was studied using response surface methodology to determine the significance levels of its influencing factors, and the optimal experimental conditions and COD removal efficiency were predicted. (ii) Investigating the effects of four factors, reaction pH, $n(H_2O_2):n(Fe^{2+})$ ratio, SPC dosage, and reaction time, on the SPC/$Fe^{2+}$ oxidation process using COD removal efficiency and chromaticity removal efficiency to determine the optimal reaction conditions and treatment effect. (iii) Using a combination of Fenton and biological activated carbon filters to treat landfill leachate. The effects of activated carbon dosage and type were investigated using COD and ammonia nitrogen removal efficiency. (iv) Developing a novel combined process of Fenton and biological activated carbon filter process to achieve efficient treatment of organic matter and ammonia nitrogen in leachate. The removal mechanism of organic matter and ammonia nitrogen by biological activated carbon filters was further studied.

## 2. Materials and methods

### 2.1. Operating conditions

The biological activated carbon column was a cylindrical container with a diameter of 15 cm and a height of 1 m. The reaction container for the influent was a cylindrical container with a diameter of 35 cm and a height of 40 cm. The two tubing tubes were made of silicone, with a length of 1 m (Fig. 1). The

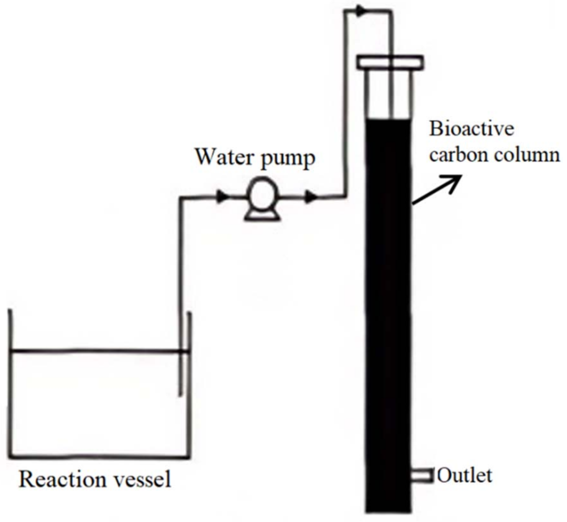

Fig. 1 Schematic of the biological activated carbon test device.

Table 1 Water quality indicators of the raw landfill leachates

| Water quality indicators | COD/mg $L^{-1}$ | $BOD_5$/mg $L^{-1}$ | $NH_4^+$-N/mg $L^{-1}$ | pH | Chromaticity |
|---|---|---|---|---|---|
| Original solution | 9885.03 | 3065.81 | 3094.81 | 8.7 | 2000 |

Table 2 Water quality indicators of the 5-fold diluted landfill leachates (measured)

| Water quality indicators | COD/mg $L^{-1}$ | $BOD_5$/mg $L^{-1}$ | $NH_3$-N/mg $L^{-1}$ | pH | Chromaticity |
|---|---|---|---|---|---|
| Stock solution (diluted five times) | 1977.01 | 613.16 | 618.96 | 8 | 400 |

test water used in this study was obtained from the equalization tank of a waste treatment plant in Shenyang City, China.

As shown in Table 1, the original COD concentration of landfill leachate from the equalization tank was as high as 9885.03 mg $L^{-1}$, which is prone to cause system instability in the early stage of the experiment. Thus, the raw leachate was diluted to explore the degradation efficiency and law of the process. To better investigate the degradation efficiency and patterns of the experimental process on the leachate, and to avoid system instability caused by excessively high concentrations of pollutants (*e.g.*, toxic inhibition on free radicals in advanced oxidation processes, or microbial inactivation in subsequent BAC tests) in the early stages of the test, the raw water was diluted 5 times with tap water for the Fenton and SPC/$Fe^{2+}$ oxidation experiments (Table 2). The same batch of diluted leachate was used for all single-factor experiments. The initial COD of each batch was determined in three parallel replicates using the dichromate method (HJ 828-2017), with the average value used as the basis for the calculation; the relative standard deviation (RSD) was less than 5%. All experiments were carried out using a 5-fold diluted leachate to avoid hydroxyl radical quenching and microbial inhibition caused by a high concentration of raw leachate.

This experiment consisted of two parts. The first part presented the Fenton advanced oxidation process for treating landfill leachate and compared it with the SPC/$Fe^{2+}$ oxidation method. The second part was the biological activated carbon filter method for treating the effluent from the first part and exploring its contribution to the removal of organic matter and ammonia nitrogen.

## 2.2. Operating conditions for Fenton advanced oxidation process

The effects of four key factors (reaction pH, $n(H_2O_2):n(Fe^{2+})$ ratio, $H_2O_2$ dosage, and reaction time) on the Fenton advanced oxidation experiment were investigated to determine the optimal operating conditions and treatment effect. The variable gradients were set based on the existing literature[27,37] and preliminary experiments, as follows: (1) pH was set to 3–8, covering the optimal pH range of the Fenton reaction (3–5) while exploring the adaptability of the process to wider pH conditions; (2) $n(H_2O_2):n(Fe^{2+})$ ratio was adjusted to 1 : 1–5 : 1 to clarify the optimal catalytic ratio of $Fe^{2+}$ for $H_2O_2$ decomposition; (3) $H_2O_2$ dosage was set to 0.5–2.5 mL (30% $H_2O_2$) to match the pollutant concentration after dilution (COD ≈ 2000 mg $L^{-1}$); and (4) reaction time was set to 20–120 min to capture the rapid oxidation stage and reaction equilibrium of the Fenton process. These variable settings ensure that the key influencing factors are fully explored while avoiding redundant gradients, improving the efficiency and accuracy of the experiment. A one-variable-at-a-time method was adopted to ensure independent adjustment of each variable, as follows: the $H_2O_2:Fe^{2+}$ molar ratio was kept constant when exploring $H_2O_2$ dosage, and the $H_2O_2$ dosage was kept constant when exploring the molar ratio. Response surface methodology was employed to investigate the Fenton oxidation process, examining the impact of multiple factors on its treatment effect. Finally, the optimal experimental conditions were analyzed and selected. The Fenton process ($H_2O_2/Fe^{2+}$) was set as system ①.

Fenton single-factor experiments were carried out *via* the one-variable-at-a-time method, with consistent basic operations, as follows: 200 mL of 5-fold diluted landfill leachate samples was added to 250 mL beakers, adjusted to the target pH with 1 mol per L sulfuric acid, followed by the addition of $FeSO_4\cdot 7H_2O$ and the corresponding oxidant, and then stirred for a set reaction time. After the reaction, COD and chromaticity were measured and analyzed. Four key factors were investigated separately.

Initial pH: pH gradient of 3.0, 4.0, 5.0, 6.0, 7.0, 8.0; fixed $n(H_2O_2):n(Fe^{2+})$ ratio of 3 : 1, $H_2O_2$ dosage of 1.5 mL, and reaction time of 60 min.

$n(H_2O_2):n(Fe^{2+})$ molar ratio: gradient of 1 : 1, 2 : 1, 3 : 1, 4 : 1, 5 : 1; fixed pH of 4.0, $H_2O_2$ dosage of 1.5 mL, and reaction time of 60 min.

$H_2O_2$ dosage: 30% $H_2O_2$ gradient of 0.5, 1.0, 1.5, 2.0, 2.5 mL; fixed pH of 4.0, $n(H_2O_2):n(Fe^{2+})$ ratio of 4 : 1, and reaction time of 60 min.

Reaction time: gradient of 20, 40, 60, 80, 100, 120 min; fixed pH of 4.0, $n(H_2O_2):n(Fe^{2+})$ ratio of 4 : 1, and $H_2O_2$ dosage of 1.5 mL.

## 2.3. Operating conditions for SPC/$Fe^{2+}$ method for treating landfill leachate

The effects of reaction pH, $n(H_2O_2):n(Fe^{2+})$ ratio, SPC dosage, and reaction time on the modified SPC/$Fe^{2+}$ oxidation experiment were investigated, focusing on changes in COD removal efficiency, color removal, and B/C ratio. SPC/$Fe^{2+}$ was set as system ②. The SPC/$Fe^{2+}$ single-factor experiments followed the same basic operation procedures as the Fenton experiments, except that 30% $H_2O_2$ was replaced with 10% SPC solution, with consistent factor gradients and fixed parameters. The corresponding SPC dosage was matched to achieve an effective oxidant content equivalent to that of the Fenton system, and the same detection indicators (COD, chromaticity, and B/C ratio) were analyzed after the reaction.

### 2.4. Operating conditions for Fenton/biological activated carbon filter combined process

**2.4.1 Operation of the activated carbon reactor.** A plastic bucket was used as the reactor, and 1 kg of fresh activated carbon was added. The 24-h day was divided into two cycles, each lasting 12 h. At the beginning of each cycle, 1 L of test water was added to the reactor. The test water was the effluent from the previous Fenton test (Table 7). The test was conducted, and at the end of each cycle, the same amount of effluent was discharged. The COD was measured, and the removal efficiency was calculated.

**2.4.2 Operation of the BAC reactor.** In the four BAC process reactors, 30 g, 100 g, and 300 g of activated carbon of type a were added to reactors A, B, and C, respectively (Table 8). The amount added to reactor D was the same as that in reactor B, 100 g, but of type b. During the operation of reactors A, B, C, and D, the influent flow rate, aeration rate, settling time, and discharge rate were maintained at consistent levels, and the reaction was carried out continuously. The COD removal efficiency was calculated by comparing the influent and effluent COD concentrations. The experimental setup was configured with influent and effluent flow rates of 1 L per cycle and a filtration rate of 4.2 m $h^{-1}$. It used effluent from the previous Fenton test (*i.e.*, landfill leachate treated by the Fenton process). The influent COD was 493.3 mg $L^{-1}$, and the sludge volume in the BAC reactor was set to 1 L.

### 2.5. Analytical methods

The analysis methods were in accordance with the water monitoring specifications and method standards promulgated by the Ministry of Environmental Protection.[53] $NH_4^+$-N (Nessler's reagent spectrophotometry using a UV spectrophotometer), COD and BOD (5-day biochemical oxygen demand), and chromaticity were analyzed according to the standard methods.[54] pH was measured using a portable pH meter (instrument: PHS-29A).

## 3. Results and discussion

### 3.1. Efficiency and optimization of the Fenton process for landfill leachate treatment

This section primarily utilizes the Fenton advanced oxidation process to treat landfill leachate. Response surface methodology was employed to investigate the Fenton process, identifying the significance levels of its influencing factors and determining the predicted optimal experimental conditions and COD removal efficiency. The Fenton process ($H_2O_2/Fe^{2+}$) was set as system ①.

**3.1.1 Treatment efficiency of the Fenton process at different pH.** As shown in Fig. 1a and b, in system ①, the removal efficiencies of both COD and chroma increase with increasing pH from 2 to 4. At pH 4, the removal efficiencies of both COD and chroma reach their maximum values of 69.60% and 95.36%, respectively, with a COD concentration of 597.06 mg $L^{-1}$ in system ①. Subsequently, with a further increase in pH, the removal efficiencies of both COD and chroma gradually decrease. Analysis of these phenomena showed that when the pH was between 2 and 4, the treatment effect gradually improved with an increasing $H^+$ concentration. When the pH value is low (<2), the high concentration of $H^+$ may lead to the formation of $[H_3O_2]^+$, which can reduce the yield of ·OH radicals.[55] When the pH gradually increased (>4), $Fe^{3+}$ reacted with $OH^-$ to form $Fe(OH)_3$ precipitate, resulting in a poor treatment efficiency. When the pH was too high, the amount of OH generated decreased, the ·OH generation rate slowed down, and the COD removal efficiency gradually decreased. It also promoted the conversion of $Fe^{2+}$ to $Fe^{3+}$, forming ferric hydroxide precipitate that led to loss of $Fe^{2+}$ catalytic activity, resulting in a negligible reaction effect. Additionally, $H_2O_2$ is unstable in an alkaline environment and readily decomposes. Therefore, both excessively low and high pH values are detrimental to the degradation of COD by Fenton's reagent. The optimal pH value was 4 (Fig. 2).

**3.1.2 Treatment efficiency of the Fenton process under different molar ratios.** It should be noted that $H_2O_2$ dosage and $H_2O_2:Fe^{2+}$ molar ratio are not mathematically independent variables. Their individual effects were investigated in single-factor experiments, and their interaction was analyzed using response surface methodology (RSM). As shown in Fig. 1c and d, in system ①, the removal efficiencies of COD and chroma reached their maximum at the $n(H_2O_2):n(Fe^{2+})$ ratio of 4 : 1, reaching 69.71% and 97.53% respectively, with a COD concentration of 599.03 mg $L^{-1}$. Further increasing the $Fe^{2+}$ concentration decreased both the COD and chroma removal efficiencies. Analysis reveals that this is primarily because a decrease in $Fe^{2+}$ concentration slows the reaction between $Fe^{2+}$ and $H_2O_2$, generating less ·OH species. As the $Fe^{2+}$ concentration continues to increase, ferric hydroxide precipitate forms, further reducing the removal efficiency. Therefore, the optimal $n(H_2O_2):n(Fe^{2+})$ ratio of 4 : 1 was chosen. We suggest that the $Fe^{2+}$ concentration is a key factor in the Fenton oxidation process. $Fe^{2+}$ accelerates the decomposition of hydrogen peroxide, acting as a catalyst, thereby enabling a high removal efficiency.

**3.1.3 Treatment efficiency of the Fenton process under different hydrogen peroxide dosages.** As shown in Fig. 1e and f, in system ①, the COD removal efficiency increased with an increasing $H_2O_2$ dosage, reaching a maximum of 74.20% at 15 mL. Afterwards, the COD removal efficiency decreased as the $H_2O_2$ dosage increased. The reason for this is that when the $H_2O_2$ content is low, increasing the $H_2O_2$ dosage results in a rapid increase in the amount of ·OH species generated over a short period, thereby accelerating the oxidation rate and enhancing the COD removal efficiency. However, when the

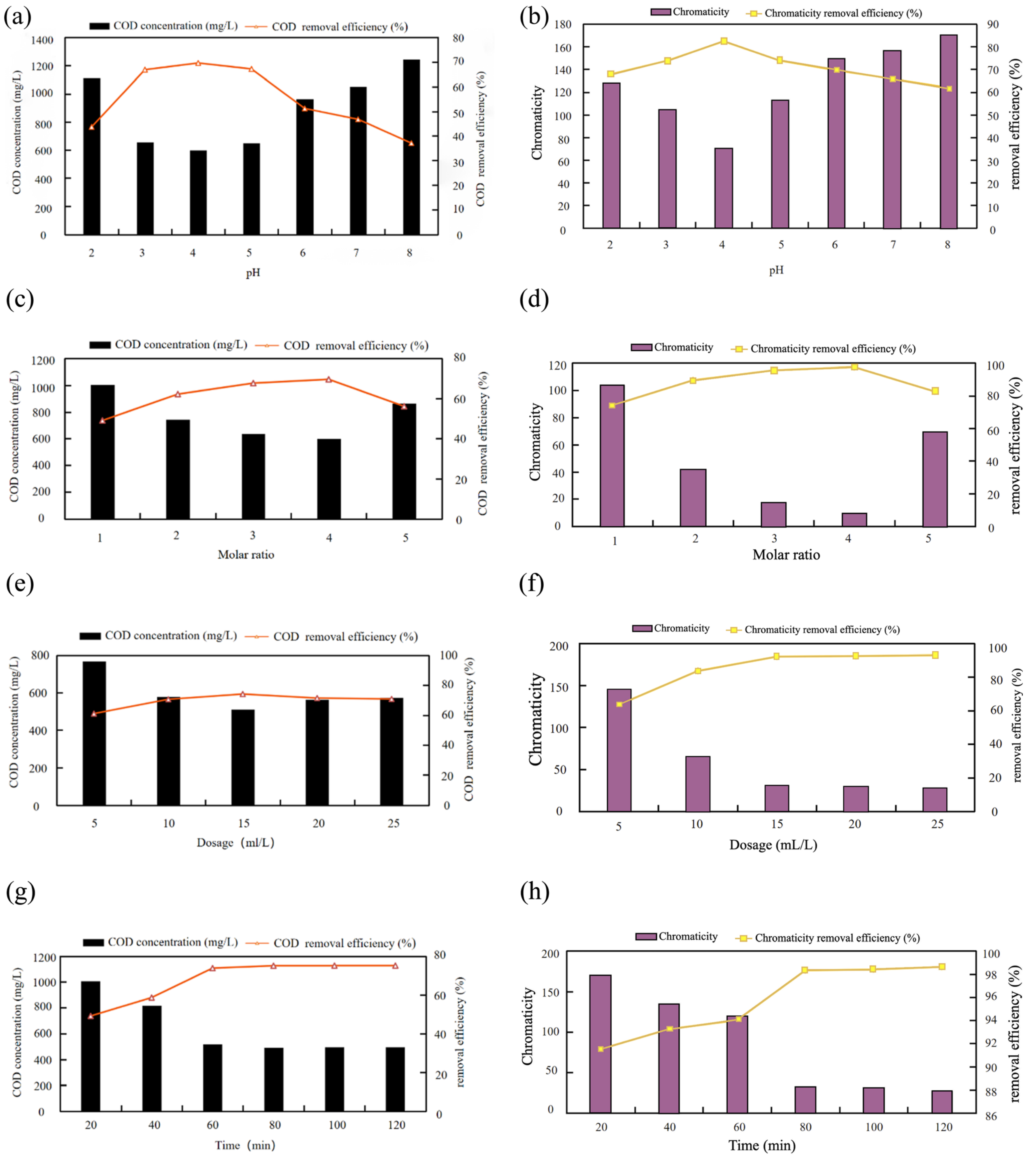

Fig. 2 Influence of the Fenton ($H_2O_2/Fe^{2+}$) systems on (a) COD removal and (b) chromaticity removal effect under different pH values; (c) COD removal and (d) chromaticity removal effect under different $n(H_2O_2):n(Fe^{2+})$ ratios; (e) COD removal and (f) chromaticity removal effect under different 30% $H_2O_2$ dosages; and (g) COD removal and (h) chromaticity removal effect under different reaction times. Left *Y*-axis: chromaticity (standard units) and right *Y*-axis: chromaticity removal efficiency (%).

$H_2O_2$ concentration in the solution reached a certain level, a further increase in the $H_2O_2$ dosage leads to excess $H_2O_2$, which accelerates its own decomposition, resulting in a decrease in the COD removal efficiency. At a $H_2O_2$ dosage of 15 mL, the COD and color removal efficiencies reached 74.20% and 92.23%, respectively, at which point the COD concentration is 510.07 mg $L^{-1}$.

**3.1.4 Treatment efficiency of the Fenton process under different reaction times.** As shown in Fig. 1g and h, in system ①, the COD removal efficiency maintained a stable upward trend until 80 min, then remained constant and slightly decreased thereafter. The COD removal efficiency reached 75.05% at 80 min, with a COD concentration of 493.26 mg $L^{-1}$. The color removal efficiency was 98.32% at 80 min. Analysis of these phenomena indicates that the Fenton reaction primarily occurs within the first 80 min and is essentially complete by then. Afterwards, the removal efficiency remains relatively unchanged. Given the time cost, the optimal reaction time was set to 80 min. Compared with existing studies,[25,31] which reported COD removal efficiencies of 65–70% for traditional Fenton processes treating landfill leachate, the COD removal efficiency of 75.1% achieved in this study is superior, which is attributed to the systematic optimization of key parameters (pH, molar ratio, and dosage) *via* single-factor experiments and RSM.

**3.1.5 Optimization of the Fenton process by the response surface method.** Based on the results of single-factor experiments, we focused on four factors: $H_2O_2$ dosage, $n(H_2O_2):n(Fe^{2+})$ ratio, pH value, and reaction time. A four-factor, three-level BBD experimental scheme was designed. The experimental data were processed and fitted using Design-Expert 8.0 to determine the optimal conditions and analyze factor interactions. Optimization is typically performed using a single factor, which overlooks interactions and prevents achieving true optimality.[55] Response surface methodology (RSM) is an effective optimization method that combines mathematical and statistical techniques to design experiments, establish and analyze models, assess the influence of factors and their interactions, and optimize conditions to achieve the ideal response.[56] Zhu *et al.*[57] used Fenton and electro-Fenton processes to treat biostabilized coking wastewater. They found that surface Fenton and electro-Fenton processes are effective for the advanced treatment of coking wastewater, and response surface methodology is suitable for their design and optimization. Virkutyte *et al.*[58] employed response surface methodology to investigate the electro-Fenton denitrification of model wastewater using platinized titanium electrodes in an electrochemical reactor. The results of the variance analysis showed that the model was statistically significant and could be used to optimize denitrification in the model wastewater. Barwal *et al.*[59] used RSM to evaluate the effectiveness of solar-Fenton photocatalytic degradation in treating heavy metals (Cu, Cd, Cr, Fe, Fi, Ni, Pb, and Zn) and pathogenic microorganisms in urban wastewater. The results showed that each variable significantly impacted the degradation of urban wastewater. Based on the RSM design principle, a BBD model was used to design a 4-factor, 3-level experiment. The experiment was represented by A, B, C, and D, as shown in Table 3, representing pH value, $n(H_2O_2):n(Fe^{2+})$ ratio, $H_2O_2$ dosage, and reaction time, respectively. The independent variables were represented by three levels: high, medium, and low, denoted by +1, 0, and −1, respectively. A total of 29 experimental points were designed, resulting in 29 sets of response surface analysis experiments. Five repetition centers were used, and COD removal efficiency was the response variable. The results of the Box–Behnken test are shown in Table 4.

Table 3 BBD experimental design factors and their levels

| | Factor | Level and coding | | |
|---|---|---|---|---|
| | | −1 | 0 | 1 |
| pH | A | 3 | 4 | 5 |
| $n(H_2O_2):n(Fe^{2+})$ ratio | B | 3 | 4 | 5 |
| $H_2O_2$ dosage (mL) | C | 10 | 15 | 20 |
| Reaction time (min) | D | 60 | 80 | 100 |

Based on the results in Tables 3 and 4, Design-Expert 8.0 was used for fitting, and a second-order empirical model was employed to represent the relationship between each factor and the removal efficiency, as shown in eqn (1) as follows:

$$Y = \beta_0 + \sum_{i=1}^{k}\beta_i X_i + \sum_{i=1}^{k}\beta_{ii}{X_i}^2 + \sum_{i=1}^{k-1}\sum_{j=i+1}^{k}\beta X_i X_j \ , \tag{1}$$

where $Y$ is the system response value; $\beta_0$ is constant term (intercept coefficient); $\beta_i$ is the linear coefficient of the independent variable $X_i$; $\beta_{ii}$ is the quadratic coefficient of the independent variable $X_i$; $\beta$ is the interaction coefficient between variables $X_i$ and $X_j$; $X_i$ and $X_j$ are the coded (or actual) values of the independent variables, which represent the main and interaction effects of each factor on the response.

Establishment of the test model and analysis of variance: by fitting the pH value, $n(H_2O_2):n(Fe^{2+})$ ratio, $H_2O_2$ dosage, and reaction time as influencing factors, and $Y$ (COD removal efficiency) as the response value, a second-order model formula was obtained. Analysis was then conducted to determine the optimal simulation conditions.

Analysis of COD removal test results: regression equation is as follows:

$$\begin{aligned} Y_{(\text{COD removal efficiency})} = {} & 74.12 + 0.90 \times A + 0.53 \times B \\ & + 0.81 \times C + 0.25 \times D + 0.12 \times A \times B \\ & + 0.30 \times A \times C + 0.075 \times A \times D \\ & + 0.20 \times B \times C - 0.10 \times B \times D \\ & - 0.025 \times C \times D - 4.97 \times A^2 \\ & - 3.09 \times B^2 - 1.16 \times C^2 - 0.80 \times D^2. \end{aligned}$$

Analysis of variance was performed on the above-mentioned second-order model, and the results are shown in Table 5.

Table 5 shows that the *F*-value for the response surface model is 28.2, and its *P*-value is less than 0.0001, indicating that this model is highly significant (the higher the *F*-value, the stronger the significance). The validation results suggest that the response surface model developed exhibits high accuracy and stability for the sample data. The *P*-value for the misfit error is 0.4029, which is greater than the significance level of 0.05, indicating that the prediction model fits the data well and is reliable. The *F*-values for pH, $n(H_2O_2):n(Fe^{2+})$ ratio, $H_2O_2$ dosage, and reaction time are 17.83, 6.07, 14.38, and 1.38, respectively. We can determine their relative influence on COD removal efficiency, *i.e.*, the significance level is pH > $H_2O_2$ dosage > $n(H_2O_2):n(Fe^{2+})$ ratio > reaction time. Therefore, the pH value has the greatest impact on Fenton oxidation and is

Table 4 BBD experimental design factors and their results

| Standard sequence | Operation sequence | A: pH | B: $n(H_2O_2):n(Fe^{2+})$ ratio | C: $H_2O_2$ dosage (mL) | D: reaction time (min) | COD removal (%) |
|---|---|---|---|---|---|---|
| 4 | 1 | 5 | 5 | 15 | 80 | 68.3 |
| 10 | 2 | 5 | 4 | 15 | 60 | 68.5 |
| 19 | 3 | 3 | 4 | 20 | 80 | 67.3 |
| 23 | 4 | 4 | 3 | 15 | 100 | 69.4 |
| 6 | 5 | 4 | 4 | 20 | 60 | 73.4 |
| 28 | 6 | 4 | 4 | 15 | 80 | 73.6 |
| 17 | 7 | 3 | 4 | 10 | 80 | 66.4 |
| 2 | 8 | 5 | 3 | 15 | 80 | 67.5 |
| 7 | 9 | 4 | 4 | 10 | 100 | 72.2 |
| 14 | 10 | 4 | 5 | 10 | 80 | 69.3 |
| 18 | 11 | 5 | 4 | 10 | 80 | 67.2 |
| 27 | 12 | 4 | 4 | 15 | 80 | 74.1 |
| 22 | 13 | 4 | 5 | 15 | 60 | 70.4 |
| 15 | 14 | 4 | 3 | 20 | 80 | 69.7 |
| 12 | 15 | 5 | 4 | 15 | 100 | 69.4 |
| 3 | 16 | 3 | 5 | 15 | 80 | 65.6 |
| 11 | 17 | 3 | 4 | 15 | 100 | 67.7 |
| 8 | 18 | 4 | 4 | 20 | 100 | 73.8 |
| 29 | 19 | 4 | 4 | 15 | 80 | 73.4 |
| 24 | 20 | 4 | 5 | 15 | 100 | 70.5 |
| 20 | 21 | 5 | 4 | 20 | 80 | 69.3 |
| 1 | 22 | 3 | 3 | 15 | 80 | 65.3 |
| 5 | 23 | 4 | 4 | 10 | 60 | 71.7 |
| 13 | 24 | 4 | 3 | 10 | 80 | 68.4 |
| 26 | 25 | 4 | 4 | 15 | 80 | 74.5 |
| 21 | 26 | 4 | 3 | 15 | 60 | 68.9 |
| 25 | 27 | 4 | 4 | 15 | 80 | 75 |
| 9 | 28 | 3 | 4 | 15 | 60 | 67.1 |
| 16 | 29 | 4 | 5 | 20 | 80 | 71.4 |

extremely important. By adjusting the appropriate pH value and setting a reasonable hydrogen peroxide dosage, molar ratio, and reaction time, the COD removal efficiency can be improved. The feasibility and goodness-of-fit of the response model are determined by $R^2$ and $R_{Adj}{}^2$, respectively. When both $R^2$ and $R_{Adj}{}^2$ are close to 1, the model has a relatively ideal fit; when they are both close to 0, the model is meaningless. Table 6 shows that $R^2$ is 0.9658 and $R_{Adj}{}^2$ is 0.9315, which suggest that this

Table 5 Variance analysis of the regression equation *Y* (COD removal efficiency)

| Source of variance | Sum of squares | Degrees of freedom | Root mean square | *F*-value | *P*-value (Prod > *F*) | Remarks |
|---|---|---|---|---|---|---|
| Model | 215.22 | 14 | 15.37 | 28.2 | <0.0001 | Significant |
| $A$ | 9.72 | 1 | 9.72 | 17.83 | 0.0009 | |
| $B$ | 3.31 | 1 | 3.31 | 6.07 | 0.0273 | |
| $C$ | 7.84 | 1 | 7.84 | 14.38 | 0.002 | |
| $D$ | 0.75 | 1 | 0.75 | 1.38 | 0.2604 | |
| $AB$ | 0.063 | 1 | 0.063 | 0.11 | 0.7399 | |
| $AC$ | 0.36 | 1 | 0.36 | 0.66 | 0.43 | |
| $AD$ | 0.023 | 1 | 0.023 | 0.041 | 0.8419 | |
| $BC$ | 0.16 | 1 | 0.16 | 0.29 | 0.5965 | |
| $BD$ | 0.04 | 1 | 0.04 | 0.073 | 0.7904 | |
| $CD$ | $2.50 \times 10^{-3}$ | 1 | $2.50 \times 10^{-3}$ | $4.59 \times 10^{-3}$ | 0.947 | |
| $A^2$ | 160.38 | 1 | 160.38 | 294.2 | <0.0001 | |
| $B^2$ | 61.73 | 1 | 61.73 | 113.24 | <0.0001 | |
| $C^2$ | 8.73 | 1 | 8.73 | 16.01 | 0.0013 | |
| $D^2$ | 4.13 | 1 | 4.13 | 7.57 | 0.0156 | |
| Residual | 7.63 | 14 | 0.55 | | | |
| Misfit error | 5.92 | 10 | 0.59 | 1.39 | 0.4029 | Not significant |
| Pure error | 1.71 | 4 | 0.43 | | | |
| Total | 222.85 | 28 | | | | |

Table 6 Model fitting results

| Statistical data | | Value |
|---|---|---|
| Standard deviation | Std dev | 0.74 |
| Average value | Mean | 69.98 |
| Coefficient of variation | CV% | 1.06 |
| Coefficient of determination | $R^2$ | 0.9658 |
| Adjusted coefficient of determination | $R_{\text{Adj}}{}^2$ | 0.9315 |
| Coefficient of determination (goodness) | $R_{\text{Pred}}{}^2$ | 0.8349 |
| Signal-to-noise ratio | Adeq. precision | 17.622 |

model simulates the real surface well; the difference between $R_{\text{Pred}}{}^2$ and $R_{\text{Adj}}{}^2$ is less than 0.2, indicating that the model has good predictive ability; the CV value is 1.06%, less than 10%, indicating that the deviation between the experimental value and the predicted value is small, and the experimental reliability is high; the signal-to-noise ratio is 17.622, which is greater than 4, indicating that the signal used in the model can be used in the model-defined space. Based on the above-mentioned experiments, pH, $n(H_2O_2):n(Fe^{2+})$ ratio, $H_2O_2$ dosage, and reaction time have significant effects on the COD removal efficiency in the Fenton process. To further investigate the influence of interactions on the response (COD removal efficiency) and to characterize the response surface, Design-Expert 8.0 was used to analyze the impact of factor interactions on the COD removal efficiency. The corresponding surface plots and contour plots were obtained. As shown in Fig. 3a and b, the degree of influence of a factor on the response value can be determined by observing the slope of the surface, where the higher and steeper the slope, the more significant the interaction between the two factors.

Furthermore, the color of the 3D plot deepens as the trend changes. The interaction between the two factors is also evident in the contour plot. As the pH value gradually increases, the effect of $n(H_2O_2):n(Fe^{2+})$ ratio on the COD removal efficiency first increases and then decreases. The impact of pH value on the COD removal efficiency is more significant than that of the $n(H_2O_2):n(Fe^{2+})$ ratio, indicating a significant interaction between the two. As shown in Fig. 3c and d, the effect of $H_2O_2$ dosage on COD removal efficiency first increases and then decreases as the pH increases gradually. The effect of pH on the COD removal efficiency is more significant than that of $H_2O_2$ dosage, and the two interact significantly. The effect of reaction time on the COD removal efficiency first increases and then decreases as the pH value increases gradually (Fig. 3e and f). The effect of pH value on the COD removal efficiency is more significant than that of reaction time. The interaction between the two is significant. The effect of $H_2O_2$ dosage on COD removal efficiency first increases and then decreases as the $n(H_2O_2):n(Fe^{2+})$ ratio gradually increases (Fig. 3g and h).

The effect of $H_2O_2$ dosage on the COD removal efficiency is more significant than that of $n(H_2O_2):n(Fe^{2+})$ ratio. The interaction between the two is significant. The effect of reaction time on the COD removal efficiency first increases and then decreases as the $n(H_2O_2):n(Fe^{2+})$ ratio gradually increases (Fig. 3i and j). The effect of $n(H_2O_2):n(Fe^{2+})$ ratio on the COD removal efficiency is more significant than that of reaction time. The interaction between the two is significant. The effect of reaction time on the COD removal efficiency first increases and then decreases as the $H_2O_2$ dosage increases (Fig. 3k and l). The $H_2O_2$ dosage has a greater impact on the COD removal

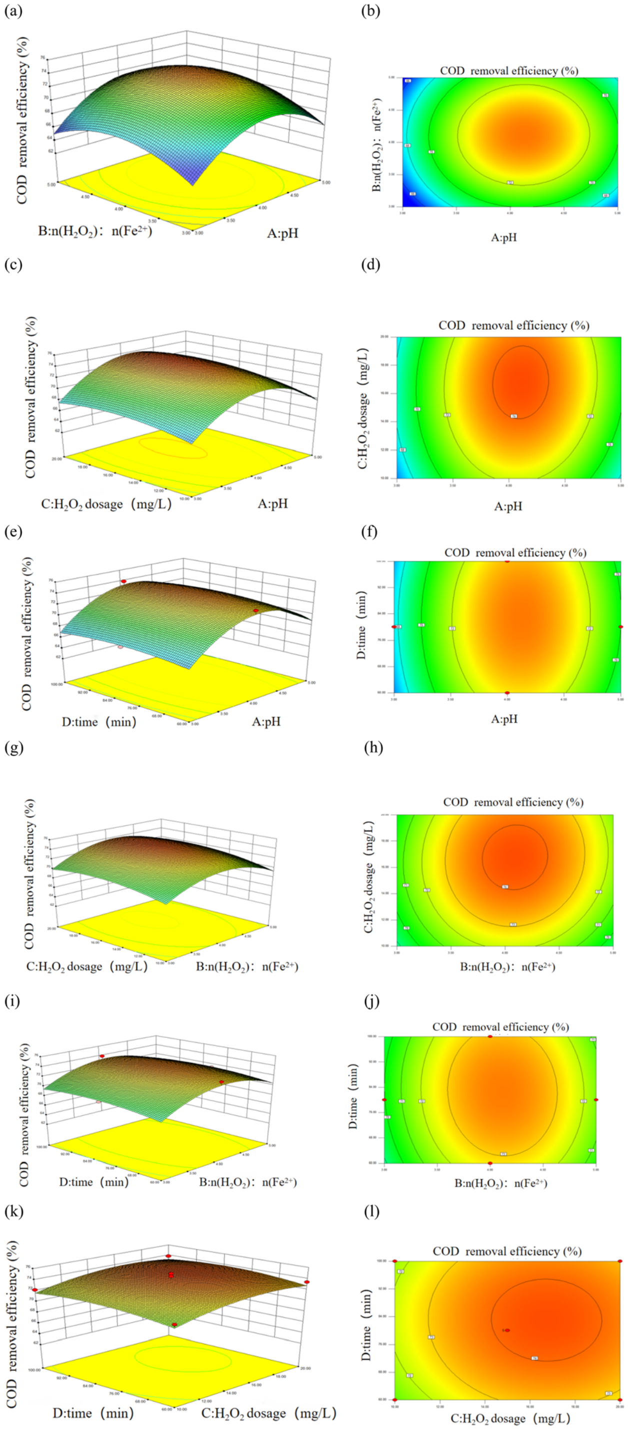

Fig. 3 Response surface and contour plots of the effects of (a) pH values and (b) $n(H_2O_2):n(Fe^{2+})$ ratios; (c) pH values and (d) $H_2O_2$ dosages; (e) pH values and (f) reaction times; (g) $n(H_2O_2):n(Fe^{2+})$ ratios and (h) $H_2O_2$ dosages; (i) $n(H_2O_2):n(Fe^{2+})$ ratios and (j) reaction times; and (k) $H_2O_2$ dosages and (l) reaction times on the COD removal efficiency.

efficiency than the reaction time. The interaction between the two is significant. The optimal conditions predicted by the software are pH 4.10, $n(H_2O_2):n(Fe^{2+})$ ratio of 4.10, $H_2O_2$ dosage of 16.84 mL $L^{-1}$, and reaction time of 83.00 min. Under these conditions, the COD removal efficiency is 74.3599%.

## 3.2. Efficiency of SPC/$Fe^{2+}$ method for treating landfill leachate

**3.2.1 Treatment efficiency of SPC/$Fe^{2+}$ process at different pH.** The removal efficiencies of both COD and color increase with increasing pH from 2 to 4. At pH 4, both the COD and color removal efficiencies reach their maximum values of 55.20% and 82.37% (Fig. 4a and b), respectively. At this point, the COD concentration is 885.70 mg $L^{-1}$. Subsequently, the removal efficiencies of both COD and color decrease gradually as the pH increases further. However, when comparing the pH range of 4–8 with system ① of the Fenton process in Section 3.1, system ② has a wider applicable pH range. Analyzing this phenomenon, SPC exhibits good water solubility and decomposes into $H_2O_2$ and $Na_2CO_3$ upon contact with water. $H_2O_2$ then begins to function, following the same principle as described in Section 3.1.1 of the Fenton experiment.

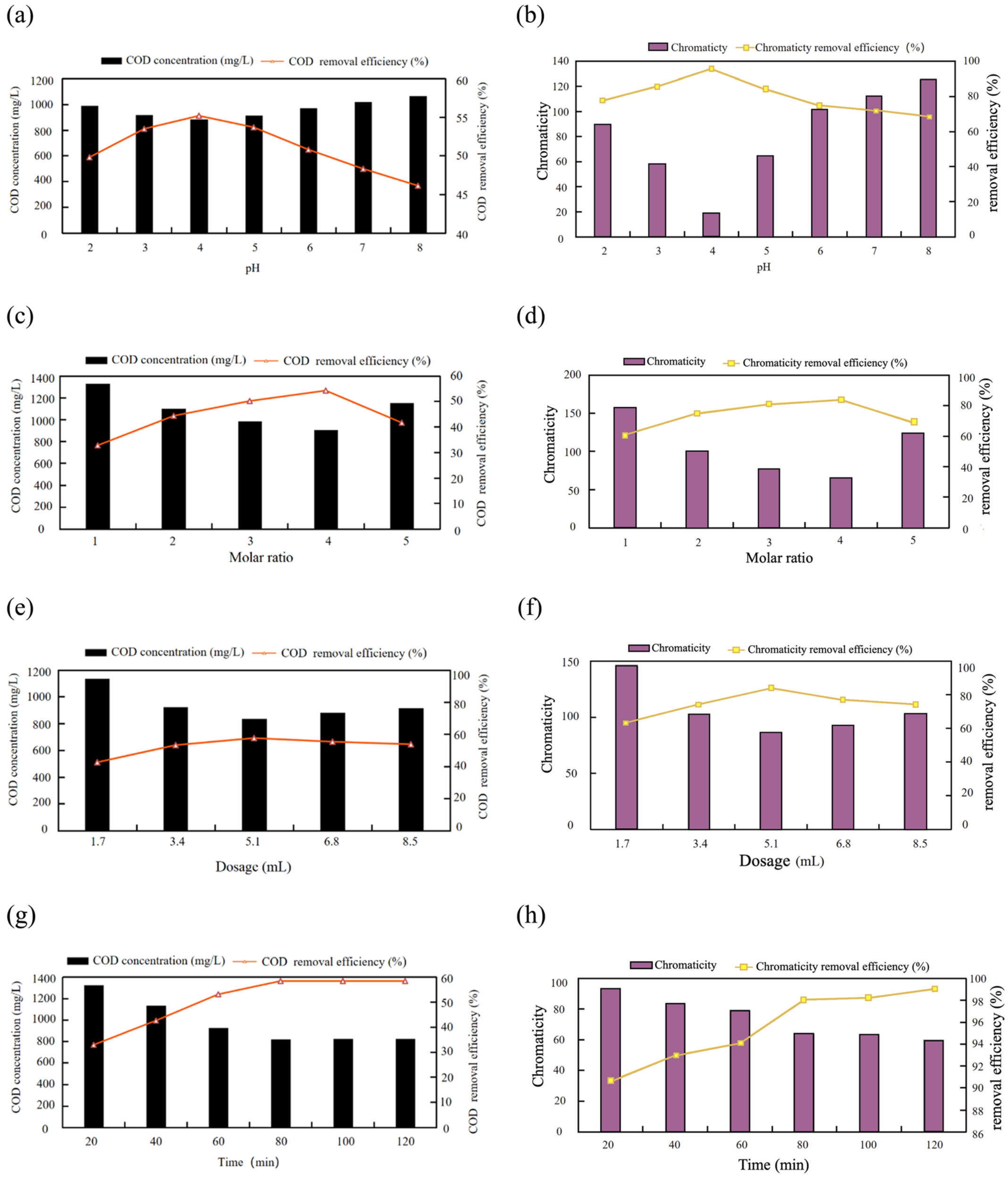

Fig. 4 Influence of the SPC/$Fe^{2+}$ systems on (a) COD removal and (b) chromaticity removal effects under different pH values; (c) COD removal and (d) chromaticity removal effects under different $n(H_2O_2):n(Fe^{2+})$ ratios; (e) COD removal and (f) chromaticity removal effects under different SPC dosages; and (g) COD removal and (h) chromaticity removal effects under different reaction times. Left Y-axis: chromaticity (standard units) and right Y-axis: chromaticity removal efficiency (%).

However, the COD removal efficiency gradually decreases at excessively high pH values, and the alkalinity of the solution increases. Because SPC has a wider applicable pH range, the decrease is slower. Therefore, the optimal pH value is 4.

**3.2.2 Treatment efficiency of the SPC/Fe$^{2+}$ process under different molar ratios.** In system ②, the removal efficiencies of COD and color reach their maximum when the $n(H_2O_2):n(Fe^{2+})$ ratio is 4 : 1, reaching 54.20% and 83.60% (Fig. 4c and d), respectively. At this point, the COD concentration is 905.47 mg L$^{-1}$. Further increasing the Fe$^{2+}$ concentration decreases both the COD and color removal efficiencies. SPC has good water solubility and decomposes into $H_2O_2$ and $Na_2CO_3$ upon contact with water. As the concentration of Fe$^{2+}$ decreases, the reaction between Fe$^{2+}$ and $H_2O_2$ slows down, generating less ·OH species. Further increasing the Fe$^{2+}$ concentration leads to the formation of ferric hydroxide precipitate with hydroxyl groups, which in turn further decreases the removal efficiency. Therefore, the optimal $n(H_2O_2):n(Fe^{2+})$ ratio is 4 : 1.

**3.2.3 Treatment efficiency of SPC/Fe$^{2+}$ process at different hydrogen peroxide dosages.** In system ②, during the initial reaction phase, the COD removal efficiency increases with an increasing SPC dosage, reaching a maximum of 57.60% at 5.1 mL (Fig. 4e and f). As the SPC dosage increases, the COD removal efficiency decreases. That is, when the dosage is 5.1 mL, the COD and color removal efficiencies are 57.60% and 83.80%, respectively, at which point the COD concentration is 838.25 mg L$^{-1}$. After dissolving in water, SPC decomposes into $Na_2CO_3$ and $H_2O_2$. $H_2O_2$ then begins to function, with organic compounds attacking, leading to a free radical scavenging effect, *etc.*, the principle of which is equivalent to that in Section 3.1.3 for the Fenton experiment.

**3.2.4 Treatment efficiency of SPC/Fe$^{2+}$ process under different reaction times.** Before 80 min, the COD removal efficiency of system ② maintained a steady upward trend (Fig. 4g and h). After that, the removal efficiency remained essentially unchanged, with a slight downward trend. When the reaction time was 80 min, the COD removal efficiency of system ② reached 58.39%, with a COD concentration of 822.44 mg L$^{-1}$ and a color removal efficiency of 84.05%. Although the maximum COD removal efficiency (58.4%) is slightly lower than that of the traditional Fenton process,[25] it is consistent with the performance of SPC/Fenton-like processes reported in the literature.[37,68] In comparison, SPC offers inherent cost advantages (62.5% of the $H_2O_2$ raw material cost) for practical applications.

### 3.3. Fenton/biological activated carbon filter combined process

Comparing the treatment efficiency of Fenton oxidation and SPC/Fe$^{2+}$ oxidation for landfill leachate, Fenton oxidation exhibits a better performance than SPC/Fe$^{2+}$ oxidation in removing COD and color from leachate. However, both methods are only moderately effective in removing ammonia nitrogen. To effectively remove ammonia nitrogen, a biological activated carbon filter is used in the later stage of the process, which has a more effective impact on ammonia nitrogen removal. The Fenton oxidation process in the early stage enhances the biodegradability of landfill leachate, thereby benefiting membrane adsorption in the later stage. The influent of the biological activated carbon filter is the effluent from the Fenton oxidation experiment in Section 3.1. The biological activated carbon filters were developed based on activated carbon. Physical adsorption and biological oxidation occur simultaneously, which significantly enhances the removal of ammonia nitrogen.[60] The biological activated carbon filters can overcome some of the shortcomings of activated carbon (AC) treatment and other conventional water treatment processes. Biological activated carbon filters use highly porous AC as a medium to immobilize microorganisms and remove organic matter from water. However, over time, the AC becomes depleted, or the adsorption sites become saturated with organic compounds. Then, microorganisms use the organic matter on the rough, porous surface of the AC medium as nutrients to multiply.

Finally, the microorganisms fill the pores and surface of the activated carbon with biomass or "biofilm". The presence of a biofilm significantly enhances the removal of organic pollutants from water.[61] Biological activated carbon filters exhibit stable, effective removal of turbidity and ammonia nitrogen in water treatment.[62,63] To overcome the low $NH_4^+$-N removal efficiency of single advanced oxidation processes, a Fenton/BAC combined process was developed using the optimal Fenton effluent (COD of 493.26 mg L$^{-1}$, B/C of 0.44, $NH_4^+$-N of 433.28 mg L$^{-1}$, and chromaticity of 6.72) as the influent. The combined process achieved an exceptional performance, with the COD removal of 81.86%, $NH_4^+$-N removal of 73.33%, chromaticity removal of 98.50%, and an increase in the B/C of the raw leachate from 0.31 to 0.51, verifying the synergistic effect of Fenton pretreatment and BAC deep treatment. This combined process outperforms existing Fenton/BAC studies,[40,68] where the COD and $NH_4^+$-N removal efficiencies were typically 70–75% and 60–65%, respectively. The improvement is due to the quantified three-level removal contributions of BAC (activated carbon adsorption-biofilm adsorption-microbial degradation) and optimized activated carbon dosage.

**3.3.1 Comparison of treatment efficiency between activated carbon adsorption and BAC reactor.** In the initial stage, the COD removal efficiency reached a maximum of 65.9%, indicating that activated carbon had a strong adsorption capacity at the beginning of the test (Fig. 5a). As the test continued, the adsorption capacity of activated carbon began to weaken. The COD removal efficiency decreased slightly. As shown in Fig. 5a, the COD change was more significant after 50 cycles and persisted through 150 cycles, during which the COD removal efficiency fluctuated considerably, averaging 26.1%. As the experiment continued, at 200 cycles, the COD removal efficiency fell below 10%, indicating that the activated carbon had reached saturation in adsorption.

The average COD removal efficiency throughout the entire experimental period was 13.7%. Fig. 5b shows the ammonia nitrogen removal efficiency during each cycle of activated carbon adsorption treatment of landfill leachate. In the initial stage, the ammonia nitrogen removal efficiency was low, but it

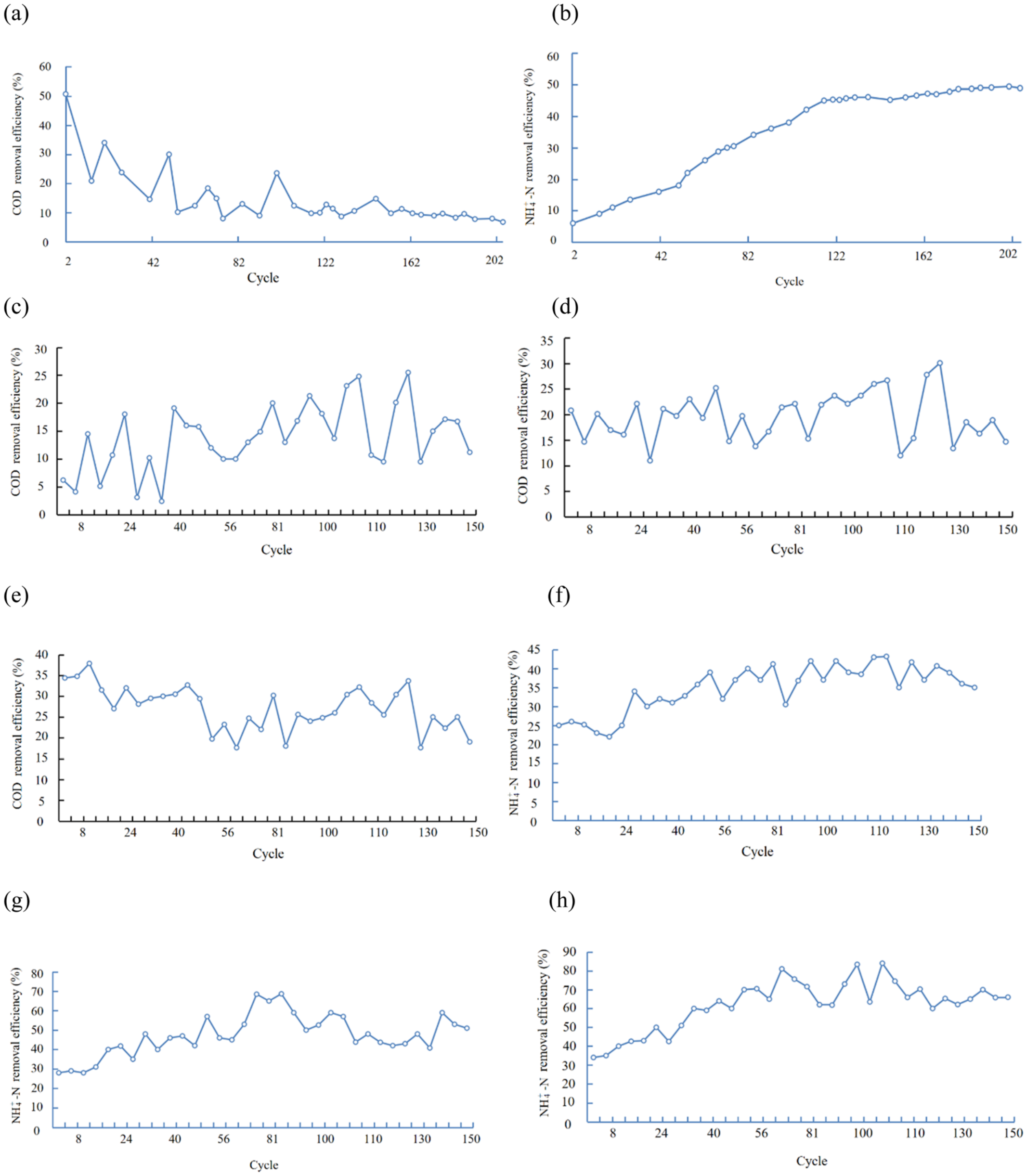

Fig. 5 Removal efficiency of (a) COD by activated carbon adsorption; (b) ammonia nitrogen from landfill leachates by activated carbon adsorption; (c) COD of reactor A in cycles 0–150; (d) COD of reactor B in cycles 0–150; (e) COD of reactor C in cycles 0–150; (f) ammonia nitrogen of reactor A in Cycles 0–150; (g) ammonia nitrogen of reactor B in cycles 0–150; and (h) ammonia nitrogen of reactor C in cycles 0–150.

increased over time, indicating that activated carbon has strong adsorption capacity. The adsorption of ammonia nitrogen in water by activated carbon involves both physical and chemical processes. The average ammonia nitrogen removal efficiency was 36.6% throughout the test period. Four BAC reactors ran continuously for 300 cycles. The average influent COD, average effluent COD, maximum and minimum COD removal efficiencies, and average COD removal efficiencies for the four BAC reactors are shown in Table 9. The average COD removal efficiencies for reactors A, B, C, and D were 13.8%, 19.6%, 27.3%, and 18.0%, respectively. The findings indicate that activated carbon adsorption was more effective in removing COD during the initial stage of the experiment. However, as the reaction progressed and adsorption continued, adsorption

Table 7 Water quality used in the test

| | COD (mg L$^{-1}$) | BOD$_5$ (mg L$^{-1}$) | NH$_3$-N (mg L$^{-1}$) | B/C | Chromaticity |
|---|---|---|---|---|---|
| Fenton effluent | 493.26 | 217.03 | 433.28 | 0.44 | 6.72 |

Table 8 Configuration of the test reactor[a]

| Reactor number | A | B | C | D |
|---|---|---|---|---|
| Activated sludge (L) | 1 | 1 | 1 | 1 |
| Activated carbon dosage (g) | 30 | 100 | 300 | 100 |
| Type of activated carbon | a | a | a | b |

[a] Type a: coal-based granular activated carbon, specific surface area = 1000–1200 $m^2\ g^{-1}$, and micropore volume = 0.45–0.50 $cm^3\ g^{-1}$. Type b: wood-based granular activated carbon, specific surface area = 300–400 $m^2\ g^{-1}$, and micropore volume = 0.10–0.15 $cm^3\ g^{-1}$.

Table 9 Average COD and COD removal efficiency of the influent and effluent from the BAC reactor over 300 cycles

| | COD average (mg $L^{-1}$) | | COD removal efficiency (%) | | |
|---|---|---|---|---|---|
| | Influent | Effluent | Maximum | Minimum | Average |
| A | 493.3 | 428.2 | 24.8 | 1.5 | 13.8 |
| B | 493.3 | 412.4 | 30.5 | 2.0 | 19.6 |
| C | 493.3 | 378.4 | 37.8 | 6.9 | 27.3 |
| D | 493.3 | 415.6 | 32.4 | 1.1 | 18.0 |

reached saturation, and the removal efficiency decreased. This indicates that the activated carbon needs to be replaced periodically for better treatment. In the BAC process, activated carbon plays two key roles: directly adsorbing pollutants and extending the contact time between organic matter and microorganisms, thereby enhancing the treatment efficiency.

### 3.3.2 Factors affecting BAC operation

*3.3.2.1 Effect of activated carbon dosage on COD and ammonia nitrogen removal efficiencies.* In three BAC reactors (A, B, and C), the same type of activated carbon was added (type a), but its dosage differed. We observed the changes in COD removal efficiencies in the three BAC reactors over the first 150 cycles under different activated carbon dosages (Fig. 5c–e). In the initial stage of the experiment, reactor C, with the highest activated carbon dosage, maintained a COD removal efficiency of around 30%. Reactor A, with a lower dosage, had a lower removal efficiency, while the removal efficiency of reactor B fell between that of A and C. This indicates that at the beginning, the adsorption capacity of activated carbon was dominant, and thus its dosage had a significant impact on the treatment effect. As the experiment continued, the adsorption capacity of the activated carbon slowly declined. During the 40-min experimental period, the COD removal efficiency of reactor C gradually decreased, and its advantage became less pronounced, dropping to around 20%. Reactor A, with its lower activated carbon dosage, was less affected by adsorption, resulting in a smaller decrease and showing minimal fluctuation. Reactor B also showed a slight decline, but its removal efficiency remained between that of reactors A and C. Therefore, in the middle stage of the BAC experiment, the impact of activated carbon dosage on the treatment effect decreased, but it remained positively correlated. During the experimental period of 60–150 cycles, the COD removal efficiency of each reactor stabilized, and adsorption also reached a steady state. Comparing the treatment effects of reactors A, B, and C under this condition, the dosage and COD removal efficiency still show a positive correlation. The activated carbon dosage remains crucial when the experiment reaches a steady state. This is because during stable operation, microbial degradation plays a dominant role. A higher amount of activated carbon helps restore greater adsorption capacity, thereby improving the COD removal efficiency and treatment effectiveness. As can be seen in Fig. 5f–h, in the initial stage of the experiment, the ammonia nitrogen removal efficiencies of the three BAC reactors were not significantly different. As the experiment progressed, the ammonia nitrogen removal efficiencies of each reactor began to increase. In the later stage of the experiment, the three BAC reactors fluctuated slightly, indicating that they had entered a stable state and that adsorption had reached a steady state. Comparing the treatment effects of reactors A, B, and C under this state, reactor C, with the largest dosage, had the highest ammonia nitrogen removal efficiency of 61.9%.

In contrast, reactor A, with the smallest dosage, had the lowest ammonia nitrogen removal efficiency of 34.8%. In BAC, the ammonia nitrogen removal efficiency is positively correlated with the activated carbon dosage. The BAC filter exhibits a superior $NH_4^+$-N removal performance, which is attributed to the enhanced oxidation capacity induced by biofilm metabolism in the filter.

*3.3.2.2 Effects of different types of activated carbon on COD and ammonia nitrogen removal in BAC.* In reactors B and D (BAC reactors), different types of activated carbon were used at the same dosage. According to the materials, the differences between the two types of activated carbon are as follows: ① surface area and ② micropore area. Activated carbon a has a surface area and micropore area that are many times higher than those of activated carbon b, by 20-times and 100-times, respectively. Based on these data, activated carbon a has stronger adsorption capacity than activated carbon b. Fig. 6a shows the COD removal efficiencies of reactors B and D. Although activated carbon a has stronger adsorption capacity than activated carbon b according to theoretical materials, their COD removal efficiencies were very close in this experiment, and activated carbon a did not show a significant advantage. Lim *et al.*[64] suggested that in the BAC reactor, the primary task of activated carbon is to adsorb toxic and harmful substances in the leachate, thereby providing a favorable environment, and to adsorb the lower COD present in the leachate. For activated carbon adsorption, the more macropores it possesses, the better the BAC treatment effect will be. In this experiment, activated carbons a and b were two different types.

The results showed that the number of micropores and the surface area of activated carbons a and b had little or no effect on the treatment effect. That is, there was no significant difference in the removal effect between different types of activated carbon. The ammonia nitrogen removal efficiency in reactor B was slightly higher than that in reactor D, indicating that the two different types of activated carbon selected have some influence on the ammonia nitrogen removal effect (Fig. 6b).

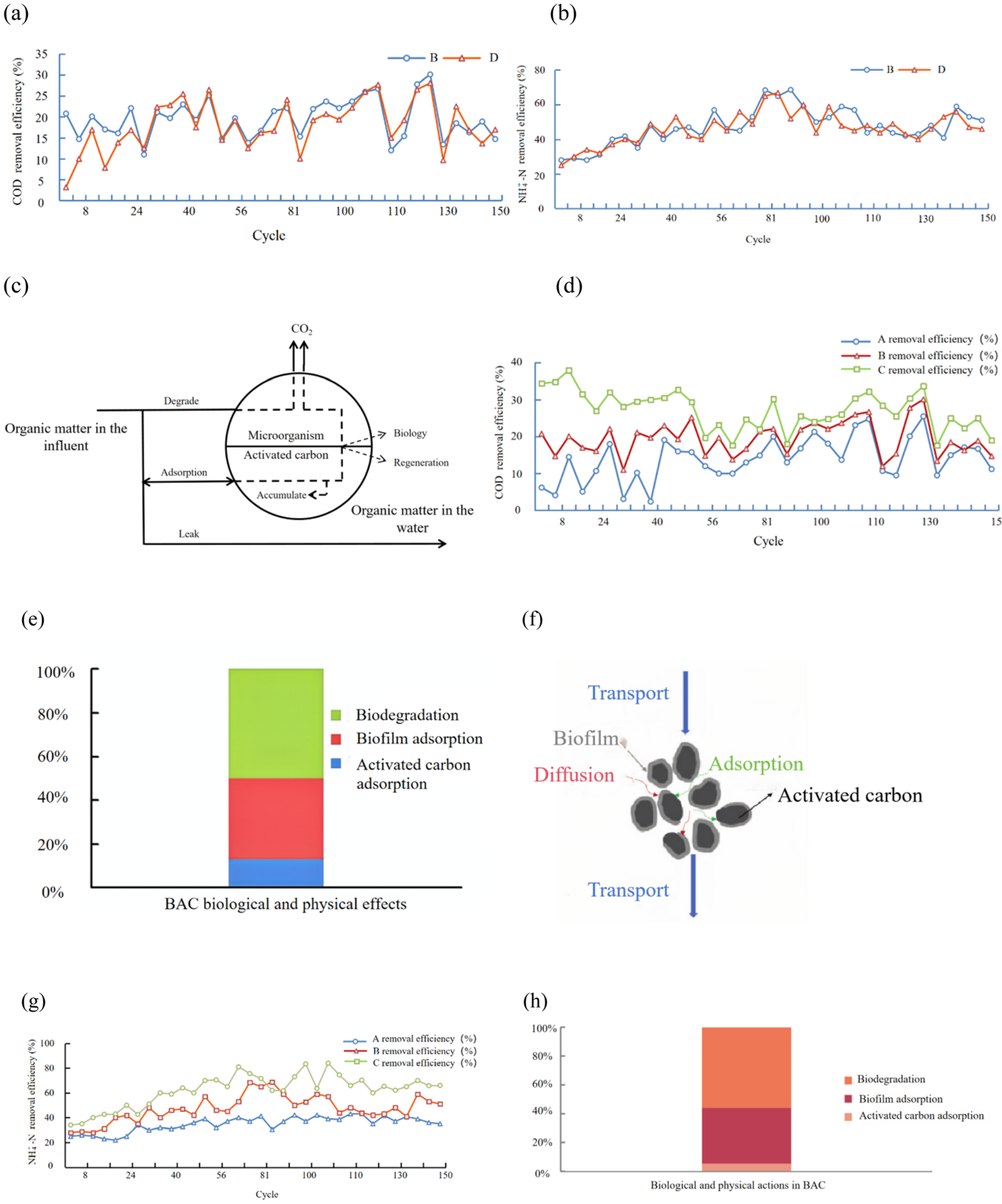

Fig. 6 (a) COD removal efficiency of the reactors B and D in cycles 0–150 and (b) ammonia nitrogen removal efficiency of the reactors B and D in cycles 0–150. (c) Schematic of the BAC process for removing organic matter. (d) COD removal efficiency of the reactors A, B, and C. (e) Percentages of the effect of BAC in COD removal mechanism. (f) Schematic of the BAC removal process of ammonia nitrogen. (g) Ammonia nitrogen removal efficiency of the reactors A, B, and C and (h) proportion of the BAC removal mechanism of ammonia nitrogen.

**3.3.3 Comparison of the contribution of BAC to the removal of organic matter and ammonia nitrogen in landfill leachate.** Different researchers use different experimental subjects, types of activated carbon, and wastewater concentrations, leading to differing conclusions. Currently, our understanding of the mechanism by which BAC removes organic matter is still incomplete. This study examines the process of removing organic matter from landfill leachate using the BAC process.

*3.3.3.1 Analysis of organic matter removal process by BAC.* Fig. 6c shows a schematic diagram of the organic matter removal process in BAC. The organic matter in the influent enters the reactor and has three possible fates: adsorption, degradation, and effluent. In the BAC reactor, organic matter undergoes both accumulation and biological regeneration reactions under the action of microorganisms and activated carbon.

① Degradation, adsorption, and effluent: organic matter enters the BAC reactor along with the influent. Microorganisms first degrade the easily degradable organic matter, generating $CO_2$, water, and inorganic matter. Simultaneously, activated carbon adsorbs some of the organic matter, while the remaining organic matter flows out with the effluent. The adsorbed organic matter accumulates and enriches on the surface of the activated carbon, eventually degrading through interactions with microorganisms, followed by biological regeneration. In the initial stage of the BAC reactor operation, adsorption plays a significant role in the entry of organic matter into the reactor, leading to a high adsorption capacity. Reactor C, with the highest activated carbon dosage, has the highest COD removal efficiency (Table 9). The COD removal efficiencies differ significantly among reactors A, B, and C when measuring the treated leachate (Fig. 5c–e, respectively). As the experiment progresses, adsorption gradually reaches saturation. The adsorption of COD begins to weaken, and its impact on the COD removal efficiency also diminishes, while microbial degradation begins to take effect. Reactor C, with the highest dosage, showed the greatest variation in COD removal efficiency and exhibited a downward trend in COD removal. Reactor A, with the lowest dosage, was less affected by adsorption and showed the smallest variation. In the later stages, we observed that the three curves slowly converged (Fig. 6d). However, upon examining the final treatment effect, the COD removal efficiency still maintained a positive correlation with the dosage.

② Accumulation and biological regeneration: organic pollutants are adsorbed onto the surface of activated carbon and accumulate. This accumulation process effectively prolongs the residence time of organic matter and the contact time with microorganisms, thereby promoting their degradation and the biological regeneration of activated carbon. In the BAC process, microorganisms primarily play the following roles: (i) degrading organic matter in wastewater and (ii) degrading organic matter adsorbed on activated carbon, helping to restore its adsorption capacity. Currently, there is no single, definitive explanation for the mechanism of bioregeneration. Nevertheless, the idea that "activated carbon can be bioregenerated under the action of microorganisms" is widely accepted. That is, bioregeneration occurs when the available sites on the activated carbon surface are depleted by adsorbed pollutants or covered by bacterial cells and extracellular polymers. The amount of activated carbon added directly affects its adsorption capacity, thus influencing the amount of biological regeneration. A certain relationship exists. Research shows a positive correlation, where the more activated carbon added, the more organic matter accumulates on its surface, providing more nutrients for microorganisms, which results in greater biodegradation, and consequently greater bioregeneration. The more activated carbon added, the greater the recoverable adsorption capacity, and the higher the COD removal efficiency. BAC degrades organic matter by extending the contact time through organic matter accumulation. Activated carbon continues to adsorb after bioregeneration. Adsorption and biodegradation mutually promote each other, maintaining the total amount of organic matter in a balanced state. Cui Yanrui *et al.*[65] measured the amount of carbon dioxide ($CO_2$) produced in a reactor aerated for 8 h. The data showed that the amount of $CO_2$ produced increased with an increase in dosage, indicating enhanced biodegradation. This indicates that the two are positively correlated. The fundamental reason recalcitrant organic matter can be biodegraded in the BAC process is biological regeneration. Sirotkin *et al.*[66] studied the adsorption and biodegradation kinetics of nonionic surfactants and found that the adsorption equilibrium of the BAC reactor was almost the same as that of general activated carbon 6 to 8 h after the start of the experiment. This indicates that at this time, biodegradation does not affect activated carbon adsorption. Adsorption and biodegradation were relatively independent before the reaction. Once adsorption reached equilibrium, the organisms were more adapted to the substrate, and the synergistic effect between the two was initiated.

3.3.3.1.1 *BAC reactor operation model.* As shown in Fig. 6c, the amount of organic matter removed in the reactor can be expressed by eqn (2), as follows:

$$a + c - e - f = b + d, \tag{2}$$

where $a$ is the organic matter content in the influent; $b$ is the organic matter content in the effluent; $c$ is the organic matter content accumulated up to the last cycle; $d$ is the organic matter content accumulated up to the current cycle; $e$ is the organic matter content that is directly degraded; $f$ is the organic matter content degraded through bioregenerative degradation; $m$ is the COD removal amount; $n$ is the biodegradable amount; and $t$ is the change in accumulated organic matter. After adjustment, we can obtain:

$$a - b - (e + f) = d - c, \tag{3}$$

$$m = a - b, \tag{4}$$

$$n = e - f, \tag{5}$$

$$t = m - n, \tag{6}$$

where $t$ is the change in accumulated organic matter in the BAC reactor over one complete cycle (mg).

(i) When $t$ is greater than 0 ($t > 0$), it indicates that the organic matter content in the BAC reactor increases over one complete cycle.

(ii) When $t$ is less than 0 ($t < 0$), it indicates that the organic matter content in the BAC reactor decreases over one complete cycle.

(iii) When the absolute value of $t$ is approximately 0, that is, $|t| \approx 0$, it indicates that the organic matter content in the BAC reactor remains essentially unchanged throughout a complete cycle. The reactor maintains a stable operating state.

(iv) When the absolute value of $t$ is large, that is, $|t|$ is large, it shows that the content of organic matter in the BAC reactor varies significantly within a complete cycle. The reactor does not maintain a stable operating state.

3.3.3.1.2 *Analysis of the BAC contribution to COD removal.* We designed and conducted synergistic mechanism experiments, and designed three small experiments, as follows:

Test ① a 12-h COD removal test was conducted using BAC, with a removal efficiency of $W_1$.

Test ② after the COD removal test in ①, the BAC was sterilized under ultraviolet light for 60 min, followed by a 12-h COD removal test, with a removal efficiency of $W_2$.

Test ③ a 12-h COD removal test was conducted using activated carbon, with a removal efficiency of $W_3$.

$$Q_1 = W_3/W_1, \tag{7}$$

$$Q_2 = (W_2 - W_3)/W_1, \tag{8}$$

$$Q_3 = (W_1 - W_2)/W_1, \tag{9}$$

where $W_1$ is the removal efficiency under the synergistic effect of the three processes; $W_2$ is the removal efficiency under the action of activated carbon and a biofilm; $W_3$ is the removal efficiency under the action of activated carbon; $Q_1$ is the percentage of activated carbon under a synergistic effect; $Q_2$ is the percentage of biofilm effect under a synergistic effect; and $Q_3$ is the percentage of microbial action under synergistic action. The obtained data were organized in this test as follows: the adsorption and removal effect of activated carbon on COD accounted for 12.5% ± 0.5%; the physical removal effect of biofilm adsorption on COD accounted for 37.5% ± 2.3%; and the biodegradation effect accounted for 50.0% ± 2.5%, as shown in Fig. 6e.

*3.3.3.2 Analysis of ammonia nitrogen removal process by BAC.* The process of removing ammonia nitrogen by BAC is similar to that of COD removal. The removal process is also related to the water flow, pollutant diffusion, and mass transfer process (Fig. 6f). During the initial stage of the BAC process operation, the physical adsorption of activated carbon plays a significant role in ammonia nitrogen removal (Fig. 6g). Reactor C, with the highest activated carbon dosage, had the highest ammonia nitrogen removal efficiency. As the experiment progressed, activated carbon adsorption reached saturation, and its adsorption of ammonia nitrogen weakened, leading to a corresponding decrease in its impact on the ammonia nitrogen removal efficiency. At this point, biofilm adsorption and biodegradation in BAC began to play a role. Reactor C, with the highest activated carbon dosage, showed the most significant variation. At the end of the cycle, the ammonia nitrogen removal efficiency was positively correlated with the dosage.

In biodegradation, bacterial nitrification plays a significant role and requires sufficient oxygen. The specific reactions are as follows:

$$\begin{aligned} 2\mathrm{NH_4}^+ + 3\mathrm{O_2} &\xrightarrow{\mathrm{AOB}} 2\mathrm{NO_2}^- + 2\mathrm{H_2O} + 4\mathrm{H}^+ \\ &- \Delta F, \quad (\Delta F = 556.84\ \mathrm{kJ}) \end{aligned} \tag{10}$$

$$2\mathrm{NO_2}^- + \mathrm{O_2} \xrightarrow{\mathrm{NOB}} 2\mathrm{NO_3}^- - \Delta F. \quad (\Delta F = 144.54\ \mathrm{kJ}) \tag{11}$$

The overall reaction is as follows:

$$\mathrm{NH_4}^+ + 2\mathrm{O_2} \rightarrow \mathrm{NO_3}^- + \mathrm{H_2O} + 2\mathrm{H}^+ - \Delta F. \quad (\Delta F = 351\ \mathrm{kJ}) \tag{12}$$

As shown in eqn (12), under normal circumstances, to ensure the regular progress of the nitrification reaction, the oxygen content in the mixed liquor in the nitrification reactor should be greater than 2.0 mg L$^{-1}$; secondly, the solution needs to maintain a specific pH and be in an alkaline state to play a buffering role. Under the condition of alkalinity (calculated as $CaCO_3$) of 7.14 g, 1 g of ammonia nitrogen can be completely nitrated.

*3.3.3.3 Analysis of the contribution ratio of BAC in removing ammonia nitrogen.* We designed and conducted synergistic mechanism experiments, and designed three small experiments as follows:

Test ① BAC removes ammonia nitrogen for 12 h, with a removal efficiency of $E_1$.

Test ② after, the BAC in Test ① is placed under ultraviolet light for 60 min for sterilization and then subjected to a 12 h ammonia nitrogen removal experiment, with a removal efficiency of $E_2$.

Test ③ activated carbon removes COD for 12 h, with a removal efficiency of $E_3$.

$$T_1 = E_3/E_1, \tag{13}$$

$$T_2 = (E_2 - E_3)/E_1, \tag{14}$$

$$T_3 = (E_1 - E_2)/E_1, \tag{15}$$

where $E_1$ is the removal efficiency under the synergistic effect of the three processes; $E_2$ is the removal efficiency under the action of activated carbon and a biofilm; $E_3$ is the removal efficiency under the action of activated carbon; $T_1$ is the percentage of activated carbon under a synergistic effect; $T_2$ is the percentage of biofilm action under a synergistic effect; and $T_3$ is the percentage of microbial action under a synergistic effect.

The obtained data were organized, and the adsorption and removal effect of activated carbon on ammonia nitrogen accounted for 5.6% ± 0.6%; the physical removal effect of biofilm adsorption on ammonia nitrogen accounted for 38.4% ± 2.3%; and the biodegradation effect accounted for 56.0% ± 2.3% (Fig. 5h). It can be seen intuitively that in the biological activated carbon filter, biodegradation plays a crucial role in removing ammonia nitrogen. Its removal mechanism is not a simple superposition of effects, but a synergistic effect of activated carbon adsorption, biofilm adsorption and microbial degradation. It can be observed that activated carbon is not sensitive to ammonia nitrogen adsorption,[67] resulting in a poor removal effect on ammonia nitrogen. Dos Santos *et al.*[68] studied the treatment of organic matter and ammonia in wastewater using biological activated carbon. They found that different types of interactions controlled bacterial attachment on the activated carbon surface. They also found that biofilm formation and bioactivity may depend on the operating conditions of the BAC process, including the quality of the injected water, backwashing state, hydraulic conditions, and temperature. Additionally, nutrient levels, carbon sources, dissolved oxygen concentration, and pH are the primary requirements for biofilm growth.

These results confirm that the Fenton/BAC combined process integrates the advantages of Fenton oxidative degradation of refractory organics (improving B/C from 0.31 to 0.51) and efficient removal of residual organics and $NH_4^+$-N by BAC, ultimately achieving 81.86% COD, 73.33% $NH_4^+$-N, and 98.50% chromaticity removal, outperforming the single Fenton (COD removal of 75.05% and $NH_4^+$-N removal of 30%) and BAC (COD removal of 27.3% and $NH_4^+$-N removal of 61.90%) processes.

### 3.4. Comparison of Fenton, SPC/$Fe^{2+}$ and Fenton/BAC processes: performance-cost analysis

The BAC process can extend the service life of activated carbon through biological regeneration,[65] reducing the replacement cost of adsorbents in long-term operation (from 0.5 USD per $m^3$ for single activated carbon to 0.15 USD per $m^3$ for BAC), thereby further improving the economic competitiveness of the combined process. Regarding the cost advantage of SPC, industrial data confirms that industrial-grade SPC (effective $H_2O_2$ content $\approx$ 14.5%) is priced at ~2000 CNY per ton, while 30% industrial $H_2O_2$ is ~800 CNY per ton; normalized to equimolar $H_2O_2$, the raw material cost of SPC is 62.5% of $H_2O_2$,[34] verifying its inherent cost benefit despite its lower treatment efficiency. From a practical perspective, firstly, the Fenton/BAC combined process is suitable for large-scale landfill leachate treatment projects (daily treatment capacity >500 $m^3$) that require deep treatment and stable discharge, as it balances high efficiency and low long-term costs. Secondly, the SPC/$Fe^{2+}$ process is more applicable to small-scale projects or remote areas due to its convenient operation and low storage risk, even with its slightly lower efficiency. Lastly, the single Fenton process is recommended only for emergency treatment scenarios (*e.g.*, sudden increases in pollutant concentration) due to its high chemical consumption and limited $NH_4^+$-N removal. This scenario-based comparison provides clear, practical guidance for selecting leachate treatment processes across different engineering cases.

## 4. Conclusion

This study proposes a Fenton/BAC combined process for efficient landfill leachate treatment. The key findings are as follows: the Fenton process exhibited a superior pretreatment performance compared to SPC/$Fe^{2+}$, achieving optimal COD, chromaticity, and $NH_4^+$-N removal efficiencies of 75.05%, 98.32%, and 30%, respectively. Response surface methodology identified pH as the most significant influencing factor, outperforming traditional Fenton studies,[25,31] which achieved only 65–70% COD removal due to the lack of systematic parameter optimization. The BAC filter achieved effective COD removal (27.3%) and excellent $NH_4^+$-N removal (61.90%) through the synergistic effects of activated carbon adsorption, biofilm adsorption, and microbial degradation. Biological regeneration was confirmed as the fundamental mechanism underlying the degradation of refractory organics by BAC. An essential mechanism that existing Fenton/BAC-related studies[40,68] failed to quantify and verify. The Fenton/BAC combined process achieved an outstanding treatment efficiency, with the COD removal of 81.86%, $NH_4^+$-N removal of 73.33%, and chromaticity removal of 98.50%. The biodegradability index (B/C) of landfill leachate increased from 0.31 to 0.51, confirming the synergistic effect of Fenton pretreatment (improving biodegradability) and BAC deep treatment (removing residual pollutants), which surpassed the reported 70–75% COD and 60–65% $NH_4^+$-N removal efficiencies of conventional Fenton/BAC processes. Notably, the process supports targeted treatment for different landfills, with adjustable Fenton parameters and BAC dosages that can be adapted to varying leachate quality, treatment scales, and economic budgets. With simple equipment, low operating costs, and easy modular transformation, it is particularly suitable for small and medium-sized landfills, and all experimental parameters are derived from actual landfill leachate treatment conditions, providing directly applicable technical parameters and process schemes for engineering implementation. The activated carbon dosage significantly affected the BAC performance, while the activated carbon type had minimal impact. A dual-dimensional analysis of performance and cost showed that the Fenton/BAC combined process had the lowest cost per unit of pollutant removal despite its slightly higher total cost, exhibiting superior overall competitiveness compared to single Fenton or SPC/$Fe^{2+}$ processes, compensating for the limitations of single performance or cost analyses in existing related studies.[34] Future research will focus on treating undiluted raw leachate, further exploring the BAC biological regeneration mechanism, and quantifying regeneration efficiency *via* $CO_2$ production measurement, thereby providing a comprehensive theoretical basis for practical application.

## Conflicts of interest

There are no conflicts of interest to declare.

## Data availability

The authors confirm that the data supporting the findings of this study are available within the article.

## Acknowledgements

The authors express their gratitude to the Liaoning Provincial Education Department Basic Research Project for Universities (Z2625128). Dr Tabassum is also thankful to the Department of Chemistry, Sakarya University.

## References

1 Z. Xianqi, *Study on Pollution Distribution and Leachate Adsorption Characteristics of a Non-standard Landfill in Northern China*, China University of Geosciences, Beijing, China, 2021.
2 C. Arteaga, J. Silva and C. Yarasca-Aybar, Solid waste management and urban environmental quality of public

space in Chiclayo, Peru, *City Environ. Interact.*, 2023, **20**, 100112.

3 L. Fangfei, *Study on Treatment of Landfill Leachate by Simultaneous Short-Cut Nitrification-Anaerobic Ammonium Oxidation-Denitrification Coupling Process (SNAD)*, North China University of Water Resources and Electric Power, Henan, China, 2022.

4 S. Islam, *et al.*, Landfill leachate a new threat to water quality: a case study from the Temperate Himalayas, *Environ. Monit. Assess.*, 2023, **195**(6), 689.

5 G. Peng, *Research on Biochemical-Physicochemical Combined Treatment Technology of Landfill Leachate at Different Landfill Stages*, Shandong University, China, 2009.

6 M. Yiming, *Study on the Environmental Pollution Risk of Soil and Groundwater Around Landfills*, Liaoning University of Engineering and Technology, Liaoning, China, 2021.

7 G. Yan, *Exploration of the Mechanism of Organic Matter Removal from Landfill Leachate by Bio-Activated Carbon*, Henan Normal University, Henan, China, 2015.

8 W. Junping, Current Status of Landfill Leachate Treatment Methods in China, *Liaoning Chem. Ind.*, 2022, **51**(11), 1580–1582.

9 Z. Jitao, in *Study on the Effect of Four-Stage Influent Anoxic/aerobic Process/hydrogen Peroxide Enhanced Iron-Carbon Micro-electrolysis Process on Leachate from Old Landfills*, Chang'an University, Shaanxi, China, 2022.

10 J. O. Alao, *et al.*, Environmental contaminants due to dumpsite leachates and the possible implications on public health, *Environ. Sci. Eur.*, 2025, **37**(1), 158.

11 M. Haili and J. Mingli, Investigation and study on heavy metal content in soil around Duyun landfill, *Resour. Conserv. Environ. Protect.*, 2016, **12**, 187–188.

12 Z. Li, *et al.*, Research progress on water quality characteristics and treatment technologies of landfill leachate, *J. Environ. Health*, 2019, **36**(6), 560–564.

13 F. Tang, G. Cao and L. Jingliang, Current status and technological progress of landfill leachate treatment in China, *J. Hebei United Univ.*, 2012, **34**(1), 5.

14 J. Zhao, Y. Li and G. J. W. Euverink, Effect of bioaugmentation combined with activated charcoal on the mitigation of volatile fatty acids inhibition during anaerobic digestion, *Chem. Eng. J.*, 2022, **428**, 131015.

15 D. R. Lima, *et al.*, Efficient acetaminophen removal from water and hospital effluents treatment by activated carbons derived from Brazil nutshells, *Colloids Surf., A*, 2019, **583**, 123966.

16 H. Susanto, *et al.*, Treatment of saline domestic wastewater using nanofiltration membrane coupled with activated carbon adsorption, *Urban Water J.*, 2022, **19**(1), 62–73.

17 H. Liang, *Study on Nitrogen Removal Performance of Landfill Leachate with Short-Cut Nitrification and Denitrification Coupled with Sludge Fermentation*, Jiangnan University, China, 2021.

18 S. Kheradmand, A. Karimi-Jashni and M. Sartaj, Treatment of municipal landfill leachate using a combined anaerobic digester and activated sludge system, *Waste Manage.*, 2010, **30**(6), 1025–1031.

19 L. Chao, *Study on the Influence of Magnetic Carriers on the Performance and Microbial Characteristics of MBBR at Low Temperature*, Inner Mongolia University of Science and Technology, China, 2022.

20 Z. Wei, *Study on the Effect of HN-AD Compound Bacteria Enhanced MBBR on Nitrogen Removal from Aquaculture Wastewater*, Chongqing Technology and Business University, China, 2022.

21 M. Pazoki, *et al.*, Attenuation of municipal landfill leachate through land treatment, *J. Environ. Health Sci. Eng.*, 2014, **12**(1), 12.

22 Q. Na, *Research on the Improvement and Application Effect of Artificial Infiltration Soil Layer for Domestic Sewage Treatment*, Beijing Forestry University, China, 2021.

23 Z. C. Wang Yu, in *Study on Removal of Tetracycline from Water by Biological Combination with UCPs-TiO2*, Nanchang University, China, 2020.

24 A. P. J. Scandelai, *et al.*, Combined processes of ozonation and supercritical water oxidation for landfill leachate degradation, *Waste Manage.*, 2018, **77**, 466–476.

25 S. Yunjian, *Study on the Efficiency of Fenton-membrane Absorption-Forward Osmosis Combined Process for Treating Landfill Leachate*, Jiangnan University, China, 2022.

26 W. Ling, *Pretreatment of High-Concentration, Recalcitrant Organic Wastewater by Iron-Carbon microelectrolysis/Fenton/flocculation Process*, Zhejiang University of Technology, China, 2010.

27 H. Weijing, *Fenton Process for Treating Leaching Wastewater from Heavy Metal Contaminated Soil [D]*, Shanghai University of Applied Technology, China, 2021.

28 Ö. Gökkuş, *et al.*, Determination of optimum conditions for color and COD removal of Reactive Blue 19 by Fenton oxidation process, *Desalin. Water Treat.*, 2014, **52**(31), 6156–6165.

29 Ö. Gökkuş and M. Oğuz, Investigation of color and COD removal by Fenton reagent from aqueous solutions containing acid and reactive dyestuffs, *Desalin. Water Treat.*, 2011, **26**(1), 160–164.

30 F. J. Rivas, *et al.*, UV-C radiation based methods for aqueous metoprolol elimination, *J. Hazard. Mater.*, 2010, **179**(1–3), 357–362.

31 P. Yiming, *Effect and Mechanism of Sodium Percarbonate (SPC) on the Control of *Anabaena Hyacinth* Blooms in Water Sources*, Shandong University, Shandong, China, 2021.

32 X. Yu, *et al.*, Synergistic effects of the combined use of ozone and sodium percarbonate for the oxidative degradation of dichlorvos, *J. Water Process Eng.*, 2021, **39**, 101721.

33 L. Li, *et al.*, Activation of sodium percarbonate by vanadium for the degradation of aniline in water: Mechanism and identification of reactive species, *Chemosphere*, 2019, **215**, 647–656.

34 X. Liu, *et al.*, A review on percarbonate-based advanced oxidation processes for remediation of organic compounds in water, *Environ. Res.*, 2021, **200**, 111371.

35 H. Xu, *et al.*, Using sodium percarbonate to suppress vertically distributed filamentous cyanobacteria while

maintaining the stability of microeukaryotic communities in drinking water reservoirs, *Water Res.*, 2021, **197**, 117111.

36 P. Li, *et al.*, Application of sodium percarbonate activated with Fe (II) for mitigating ultrafiltration membrane fouling by natural organic matter in drinking water treatment, *J. Cleaner Prod.*, 2020, **269**, 122228.

37 X. Fu, *et al.*, Benzene depletion by Fe2+-catalyzed sodium percarbonate in aqueous solution, *Chem. Eng. J.*, 2015, **267**, 25–33.

38 X. Zang, *et al.*, Trichloroethylene oxidation performance in sodium percarbonate (SPC)/Fe2+ system, *Environ. Technol.*, 2014, **35**(7), 791–798.

39 X. Yingying, *Study on the Adsorption Efficiency and Mechanism of Malachite Green Based on Manganese Modified Activated Carbon*, Shandong Jianzhu University, Shandong, China, 2022.

40 L. Bulin, *Research on the Water Purification Efficiency and Operation Control of BAC Based on Biofunctional Regulation*, Guangdong University of Technology, Guangdong, China, 2022.

41 A. A. Cuthbertson, *et al.*, GAC to BAC: does it make chloraminated drinking water safer?, *Water Res.*, 2020, **172**, 115432.

42 S. Dong, *et al.*, Occurrence and succession of bacterial community in O3/BAC process of drinking water treatment, *Int. J. Environ. Res. Public Health*, 2019, **16**(17), 3112.

43 M. Dhadwal, Y. Liu and B. R. Dhar, Coupling microbial electrolysis cell and activated carbon biofilter for source-separated greywater treatment, *Processes*, 2021, **9**(2), 281.

44 W.-L. Wang, *et al.*, Combination of catalytic ozonation by regenerated granular activated carbon (rGAC) and biological activated carbon in the advanced treatment of textile wastewater for reclamation, *Chemosphere*, 2019, **231**, 369–377.

45 E. Schneider, A. Cerqueira and M. Dezotti, MBBR evaluation for oil refinery wastewater treatment, with post-ozonation and BAC, for wastewater reuse, *Water Sci. Technol.*, 2011, **63**(1), 143–148.

46 X. Jiang, *et al.*, Adsorption of COD in Coking Wastewater on Nitric Acid-Modified Blue Coke Activated Carbon, *J. Chem.*, 2019, **2019**(1), 8593742.

47 J. L. Shi and D. L. McCurry, Transformation of N-methylamine drugs during wastewater ozonation: formation of nitromethane, an efficient precursor to halonitromethanes, *Environ. Sci. Technol.*, 2020, **54**(4), 2182–2191.

48 L. Dong, *et al.*, Research on the application potential of spent biological activated carbon from BAC process to remove radionuclides Sr2+ from water, *J. Radioanal. Nucl. Chem.*, 2021, **327**(3), 1179–1190.

49 P. Gandi, *Study on the Spatial Distribution Characteristics of Typical Extracellular Enzymes in EPS during Wastewater Biological Treatment*, Guangzhou University, Guangzhou, China, 2021.

50 Q. Jiang, *et al.*, Pilot-scale and mechanistic study of the degradation of typical odors and organic compounds in drinking water by a combined UV/H2O2-BAC process, *Chemosphere*, 2022, **292**, 133419.

51 K. I. A. Hamid, *et al.*, Comparison of the effects of ozone, biological activated carbon (BAC) filtration and combined ozone-BAC pre-treatments on the microfiltration of secondary effluent, *Sep. Purif. Technol.*, 2019, **215**, 308–316.

52 Y. Kim and K. Hyun, Performance assessment on combined process of the oxidation and Biological Activated Carbon filtration for removal of Chlorinated Volatile Organic Carbons from river water, *KSCE J. Civ. Eng.*, 2018, **22**(1), 46–53.

53 The Editorial Board of State Bureau of Environmental Protection, *Water and Wastewater Monitoring Analysis Method*, Environmental Science Press, Beijing, China, 4th edn, 2002, vol. 88–439, p. 448.

54 A. D. Eaton, *et al.*, *Standard Methods for the Examination of Water & Wastewater*, American Public Health Association, American Water Works Association, Water Environment Federation, 2005.

55 L. Cohen, M. D. Willis and K. R. Wilson, Iron (IV) formation and the pH dependent Kinetics of the Fenton reaction, *Angew. Chem.*, 2025, **137**(49), e17261.

56 H. Yunzheng, *Research on the Optimization of Design Parameters of Tuned Mass Damper Based on Response Surface Method*, Kunming University of Science and Technology, Yunnan, China, 2022, pp. 12–20.

57 X. Zhu, *et al.*, Optimization of Fenton and electro-Fenton oxidation of biologically treated coking wastewater using response surface methodology, *Sep. Purif. Technol.*, 2011, **81**(3), 444–450.

58 J. Virkutyte, E. Rokhina and V. Jegatheesan, Optimisation of Electro-Fenton denitrification of a model wastewater using a response surface methodology, *Bioresour. Technol.*, 2010, **101**(5), 1440–1446.

59 A. Barwal and R. Chaudhary, Effectiveness of Solar Photo-Fenton Process for Simultaneous Detoxification of Heavy Metals and Disinfection in Municipal Wastewater by Using Response Surface Method, *Environ. Prog. Sustainable Energy*, 2017, **36**(2), 448–459.

60 J. Ruiqi, *Laboratory Study on Treatment of Aged Leachate by Powdered Activated Carbon Anoxic Biofilter/SBR Combined Process*, Nanjing University, Jiangsu, China, 2019, pp. 17–25.

61 F. Xiaolin, *Performance and Microbial Analysis of Low-Temperature Ammonia Nitrogen Removal in Iron-Enhanced Biological Activated Carbon Filters*, Hebei University of Technology, Hebei, China, 2020, pp. 36–47.

62 E. M. Aieta and J. D. Berg, A review of chlorine dioxide in drinking water treatment, *J.–Am. Water Works Assoc.*, 1986, **78**(6), 62–72.

63 M.-Y. Xu, *et al.*, Chlorine dioxide-based oxidation processes for water purification:A review, *J. Hazard. Mater.*, 2022, **436**, 129195.

64 P.-E. Lim, *et al.*, Treatment of landfill leachate in sequencing batch reactor supplemented with activated rice husk as adsorbent, *Chem. Eng. J.*, 2010, **159**(1–3), 123–128.

65 C. Yanrui and G. Yan, *Efficient Removal of Organic Matter from Landfill Leachate by Bio-Activated Carbon*, Proceedings of the

Annual Academic Conference of Henan Chemical Society, Henan People's Publishing House, Henan, 2014, p. 358.

66 A. S. Sirotkin, L. Y. Koshkina and K. G. Ippolitov, The BAC-process for treatment of waste water containing non-ionogenic synthetic surfactants, *Water Res.*, 2001, **35**(13), 3265–3271.

67 S.-H. Kim and M. Pirbazari, Bioactive adsorber model for industrial wastewater treatment, *J. Environ. Eng.*, 1989, **115**(6), 1235–1256.

68 P. R. Dos Santos and L. A. Daniel, A review: organic matter and ammonia removal by biological activated carbon filtration for water and wastewater treatment, *Int. J. Environ. Sci. Technol.*, 2020, **17**(1), 591–606.